NACA TN No. 1789

8235

TECH LIBRARY KAFB, NM
0144820

NATIONAL ADVISORY COMMITTEE FOR AERONAUTICS

TECHNICAL NOTE

No. 1789

INVESTIGATION OF AERODYNAMIC AND ICING CHARACTERISTICS OF RECESSED FUEL-VENT CONFIGURATIONS

By Robert S. Ruggeri, Uwe von Glahn
and Vern G. Rollin

Lewis Flight Propulsion Laboratory
Cleveland, Ohio

Washington
March 1949

TECH
AFL 2611

319.98/91

TECH LIBRARY KAFB, NM
0144820

NATIONAL ADVISORY COMMITTEE FOR AERONAUTICS

TECHNICAL NOTE NO. 1789

INVESTIGATION OF AERODYNAMIC AND ICING CHARACTERISTICS OF RECESSED FUEL-VENT CONFIGURATIONS

By Robert S. Ruggeri, Uwe von Glahn
and Vern G. Rollin

SUMMARY

An investigation has been conducted in the NACA Cleveland icing research tunnel to determine the aerodynamic and icing characteristics of several recessed fuel-vent configurations. The vents were investigated aerodynamically to obtain vent-tube pressures and pressure distributions on the ramp surface as functions of tunnel-air velocity and angle of attack. Icing investigations were made to determine the vent-tube pressure losses for several icing conditions at tunnel-air velocities ranging from 220 to 440 feet per second.

In general, under nonicing conditions, the configurations with diverging ramp walls maintained vent-tube pressures greater than the required marginal value of 2 inches of water positive pressure differential between the fuel cell and the compartment containing the fuel cell for a range of angles of attack from 0° to 14° at a tunnel-air velocity of approximately 240 feet per second. A configuration having diverging ramp sidewalls, a 7° ramp angle, and vent tubes manifolded to a common plenum chamber opening through a slot in the ramp floor gave the greatest vent-tube pressures for all the configurations investigated. The use of the plenum chamber resulted in uniform pressures in all vent tubes.

In a cloud-icing condition, roughness caused by ice formations on the airfoil surface ahead of the vent ramp, rather than icing of the vent configuration, caused a rapid loss in vent-tube pressures during the first few minutes of an icing period. Only the configuration having diverging ramp sidewalls, a 7° ramp angle, and a common plenum chamber maintained the required vent-tube pressures throughout a 60-minute icing period, although the ice formations on this configuration were more severe than those observed for the other configurations. No complete closure of vent-tube openings occurred for the configurations investigated.

A simulated freezing-rain condition caused a greater and more rapid vent-tube pressure loss than was observed for a cloud-icing condition.

INTRODUCTION

1033

Several types of fuel cell now in use in transport airplanes tend to collapse under negative pressure, venting in such a manner that much of the contents is expelled. Overpumping during fuel transfer between cells may also cause the fuel to be expelled through the vents. The location of fuel-cell vents is very important in the reduction of fire hazards because fuel expelled from improperly located vents may seep into the wings or the fuselage proper and thereby create a serious fire hazard.

The existence of a negative pressure in a fuel cell may be eliminated by proper sealing of the fuel-cell compartment and by venting the compartment to the upper wing surface while venting the fuel cell to the lower surface. This solution, however, is impractical for many existing fuel-cell installations because of structural difficulties.

In order to minimize the fire hazard, the vents can be relocated from the fuselage and the nacelles to the lower surface of the outer wing panels. Because this location of the vents is in an area susceptible to icing, particularly during high angle-of-attack attitudes, it was necessary to determine whether ice formations would sufficiently impair the aerodynamic characteristics of the vent to cause failure of the fuel cells.

In a previous study of ice-free vents consisting of bent tubes facing downstream (reference 1), the fuel-tank pressures were in the order of $-0.1\ q_0$ (where q_0 is the free-stream velocity pressure). Because of its negative-pressure characteristics, this type of vent cannot be utilized with collapsible fuel cells.

In an effort to obtain an ice-free vent that would provide a positive pressure in the fuel cell with respect to the fuel-cell compartment, several recessed vent configurations were investigated in the icing research tunnel of the NACA Lewis laboratory to determine the aerodynamic and icing characteristics. A positive pressure

1033

differential of 2 inches of water between the interior of the fuel cell and the compartment containing the fuel cell was considered marginal for satisfactory operation of fuel cells. This criterion was used to evaluate the merits of the vent configurations. The vent pressure characteristics were obtained as a function of angle of attack and tunnel-air velocity for both dry and icing conditions.

APPARATUS AND INSTRUMENTATION

The investigation to determine the icing and pressure characteristics of recessed fuel-vent configurations was conducted in the 6- by 9-foot test section of the Lewis icing research tunnel. The vent configurations were fabricated of aluminum and were mounted on an NACA 65,2-216, $a = 1.0$, airfoil section of 8-foot chord (fig. 1) so that the rear wall of the vents was located on the lower surface of the airfoil at 67 percent of chord. The leading edge of the airfoil section was equipped with an external electric heater extending aft to 20 percent of chord and heat could be selectively applied to any given chord length up to the limits of the heater.

Description of Vent Configurations

The vent configurations used in the investigation are shown in figures 2 and 3.

Configuration A. - The first configuration investigated consisted of vent-tube openings submerged below the surface of a wing. The sidewalls of the vent ramp were approximately parallel. The ramp floor was curved and the mean ramp angle (fig. 3(a)) was relatively large in order to minimize structural changes in existing wings. Three vent tubes $1\frac{1}{4}$ inches in diameter (tubes 1, 3, and 4, fig. 2(a)) and one vent tube 1 inch in diameter (tube 2, fig. 2(a)) were mounted flush in the rear slope of the recess and each tube was manifolded to a common outlet on the upper surface of the airfoil (fig. 4). The pressure differential between the upper and lower surfaces of the airfoil section was used to induce air flow through the vent tubes. A plate of chamfered sheet aluminum 1/32 inch thick was installed on the wing surface aft of the vent tubes to represent the skin of a typical installation. This plate was used only with configuration A.

1033

Configuration B. - The second configuration investigated was similar to configuration A with respect to ramp sidewalls, ramp angle, and curvature (fig. 3(a)).

Three vent tubes $1\frac{1}{4}$ inches in diameter (tubes 1, 2, and 4, fig. 2(b)) and one vent tube 1 inch in diameter (tube 3, fig. 2(b)) were mounted in the ramp floor in the region of maximum recess ($1\frac{1}{16}$ in. with respect to wing surface) with the tubes normal to the wing surface.

Configuration C. - The third configuration investigated had curved diverging ramp sidewalls (fig. 2(c)) and was based on recent submerged-inlet studies conducted at the NACA Ames laboratory. The coordinates for the sidewall divergence are given in table I. The ramp angle for this configuration was 5° and the ramp floor proper had no curvature. Because the point of maximum recess was maintained the same as configurations A and B whereas the ramp angle was decreased, the over-all chordwise length of this vent was approximately doubled as compared with configurations A and B. The vent tubes were located in the ramp floor in the region of maximum recess and were mounted normal to the wing surface, as shown in figure 3(b). The vent-tube diameters and locations with respect to each other were similar to those of configuration A.

Configuration D. - The fourth configuration investigated was similar to configuration C with respect to ramp sidewall divergence, ramp angle, and ramp floor (fig. 3(b)). Four vent tubes were mounted flush in the rear slope of the recess. The vent tube diameters and locations with respect to each other were similar to those of configuration A.

Configuration E. - The final configuration investigated had curved divergent ramp sidewalls (fig. 2(d)) and was also based on recent submerged-inlet studies conducted at the Ames laboratory. The coordinates for the sidewall divergence of this configuration are also listed in table I. The ramp angle was 7° and the ramp floor had no curvature. The point of maximum recess was increased from $1\frac{1}{16}$ to $1\frac{5}{16}$ inches. Four vent tubes, each $1\frac{1}{4}$ inches in diameter, were manifolded to a plenum chamber, one side of which formed a slot 1 by 4 inches in the ramp floor at the point of maximum recess, as shown in figures 2(d) and 3(c). The vent tubes were located on the upstream side of the plenum chamber and were staggered with respect to each other in order to reduce the width of the slot. The plenum chamber was 5 inches deep.

1033

Measurements

The air flow through the vent lines was measured by a calibrated orifice installed in each vent tube. The flow of air through the tubes was controlled by means of a valve installed in each vent line. Vent-tube static pressure was measured at a point 1 inch from the tube opening on the upstream surface of the tubes. Nine surface static-pressure measurements were made along the center line of the vent ramps by means of flush-type static-pressure tubes. For configuration E, four additional static-pressure tubes were located spanwise across the rear slope of the vent, as shown in figure 2(d). All pressure readings were photographically recorded from multiple manometers.

A water trap was installed in one of the $1\frac{1}{4}$-inch vent tubes of configuration A in order to collect and measure water entering the vent tube in a simulated-rain condition.

EXPERIMENTAL TECHNIQUES AND PROCEDURE

Aerodynamic. - In order to determine the aerodynamic characteristics of the vent configurations, static-pressure distributions on the vent-ramp surface were obtained for a range of tunnel-air velocities from approximately 220 to 400 feet per second with no air flow through the vent tubes and for a range of measured angles of attack from 0° to 12°. Vent-tube static pressures were obtained as a function of angle of attack and tunnel-air velocity. The aerodynamic characteristics of the vents were also determined with an air flow of approximately 0.6 pound per minute through the large vent tubes and a correspondingly decreased air flow through the small vent tube. These values of air flow through the tubes represented a simulated descent in altitude at the rate of 3000 feet per minute.

Rain. - An investigation to determine the amount of liquid water that would be admitted into the vent lines of configuration A was made under a simulated rain condition with an air flow of 0.6 pound per minute through the large vent tubes, a tunnel-air velocity of 220 feet per second, an ambient-air temperature of 46° F, and a measured angle of attack of 14°. The liquid-water content was approximately 4.5 grams per cubic meter. The droplet size was considerably larger than 20 microns and was estimated to be of the order of 50 microns. This droplet size, usually considered a fine drizzle, was the largest obtainable with the spray system used in the investigation.

1033

Icing. - The cloud-icing characteristics of the vent configurations were determined for measured angles of attack ranging from 3° to 14° and at tunnel-air velocities ranging from approximately 470 to 220 feet per second, respectively. The investigations were conducted at high angles of attack in order to subject the vents to the maximum direct water impingement. The liquid-water content for the cloud-icing conditions ranged from 0.6 to 1.5 grams per cubic meter and varied inversely with tunnel-air velocity. The droplet size, as determined by volume maximum, ranged from approximately 15 to 25 microns. Both liquid-water content and droplet size were determined by the rotating-cylinder technique. These cloud-icing conditions were the most severe that could be obtained with the spray system used in the investigations.

Measurements of vent-tube air flow and static pressure were obtained throughout the cloud-icing periods. The vent air flow at the beginning of a cloud-icing period ranged from 0.5 to 0.65 pound per minute through the large vent tubes.

With the exception of configuration C, the vent configurations were also investigated for a simulated freezing-rain condition at ambient-air temperatures ranging from 20° to 23° F. The liquid-water content for these experiments ranged from 0.7 to 1.8 grams per cubic meter with a droplet size larger than 20 microns and estimated to be in the order of 50 microns. The experiments were made at tunnel-air velocities of approximately 220 to 400 feet per second at measured angles of attack of 14° and 3°, respectively. At the beginning of the freezing-rain periods, the vent-tube air flow was approximately 0.6 pound per minute.

During the icing investigations, including both cloud icing and freezing rain, the leading edge of the airfoil was maintained ice-free for 10 to 15 percent of chord, except as noted in the discussion.

Tunnel corrections. - The free-stream velocity and static pressures and the angle of attack of the airfoil section were corrected for tunnel-wall and model-blocking effects by the method of reference 2. Because the measured lift, drag, and moment coefficients for the airfoil used in the investigation were unavailable, typical values for these coefficients were assumed from corrected data available on an NACA 65,2-215, a = 0.5, airfoil and used in the equations given in reference 2. During the icing investigations, the data were corrected for conditions existing at the beginning of the icing periods, and these conditions and corrections were assumed to remain the same throughout the icing period.

The corrected angles of attack based on the assumed lift and moment coefficients are within $\pm 0.5^{\circ}$ of the true values. Because the drag coefficients at angles of attack below 16° influence the free-stream velocity and static-pressure corrections only to a minor degree, the corrected pressure values presented based on assumed coefficients are considered conservative and within the experimental error.

RESULTS AND DISCUSSION

All airfoil angles of attack and vent-tube pressure characteristics presented hereinafter in the aerodynamic and icing investigations are corrected for tunnel-wall and blocking effects.

Aerodynamic

Ramp-surface-pressure distribution. - The variation of ramp-surface pressure with angle of attack for the five configurations investigated is shown in figure 5. The surface pressures are presented in terms of the pressure coefficient $\frac{p-p_0}{q_0}$, where p is the surface static pressure, p_0 is the corrected free-stream static pressure, and q_0 is the corrected free-stream velocity pressure. In general, the local static surface pressure coefficients at the beginning of the vent ramp are negative even at an angle of attack of approximately 14°. The maximum positive surface pressure at a given angle of attack occurred on the rear slope of the recess for all configurations. The vent tubes of configurations A and D were located in the region of maximum pressure. A high surface pressure at a given angle of attack was also obtained in the region of maximum recess in which the vent-tube openings of configurations B and C and the plenum-chamber slot of configuration E were located. As the angle of attack was increased, the surface pressures became more positive for all configurations investigated.

Vent-tube pressure characteristics. - The variation of vent-tube pressures with angle of attack (fig. 6) is presented in terms of the corrected free-stream velocity pressure as $\frac{p_s-p_0}{q_0}$, where p_s is the static pressure measured 1 inch inside the tube opening. In general, the vent-tube pressures increased rapidly with increasing angles of attack. Investigations showed that the variation of the pressure in the vent tubes was negligible for conditions of no air flow to an air flow of 0.6 pound per minute through the vent tubes.

For configuration A, the marginal vent-tube pressure differential p_s-p_0 of 2 inches of water positive pressure between a fuel cell and a compartment containing the fuel cell was reached at an angle of attack of 4° for a tunnel-air velocity of 240 feet per second, (q_0, 13.2 in. water)(fig. 6). On this basis, it appears that this configuration is marginal for normal nonicing flight conditions.

The marginal vent-tube pressure for configuration B was attained at an angle of attack of 6° at a tunnel-air-velocity of 240 feet per second (q_0, 13.1 in. water), as can be determined from figure 6. At a higher tunnel-air velocity of 370 feet per second (q_0, 29.7 in. water), the marginal vent-tube pressure was reached at an angle of attack of 1°. The results of the investigation of this configuration show that the configuration is submarginal for normal nonicing flight conditions.

The variation of vent-tube pressure as a function of angle of attack in figure 6 for configuration C is for a tunnel-air velocity of 240 feet per second (q_0, 13.0 in. water). All vent tubes maintained a satisfactory vent-tube pressure for all angles of attack investigated. The vent-tube pressures of tubes 1 and 4, however, were somewhat less than those observed for tubes 2 and 3. The difference between the inner and outer vent-tube pressures is caused by the close proximity of the ramp sidewalls to the outer tubes and the divergence of these walls. The vent configuration is satisfactory for normal nonicing flight conditions.

For configuration D, the variation of vent-tube pressure with angle of attack in figure 6 is for a tunnel-air velocity of 240 feet per second (q_0, 13.2 in. water). Satisfactory vent-tube pressure differentials p_s-p_0 were obtained at all angles of attack investigated. The vent-tube pressure characteristics were similar to those of configuration C in that the outer vent tubes showed a decreased pressure as compared with the inner vent tubes.

Results of investigations with configurations C and D and submerged-inlet studies at the Ames laboratory indicated that a spanwise pressure gradient across the rear slope existed and resulted in increased vent-tube pressures for the center tubes as compared with the outer tubes. In an effort to utilize this high-pressure region for all the vent tubes, and at the same time maintain approximately the same overall vent dimensions, configuration E was designed with a slot opening spanning this high-pressure region. It was determined that the ratio of the slot width to maximum vent width should not exceed 0.55, as shown in figure 7. The effect of the plenum chamber together with the relatively uniform pressure gradient across the slot permits all the vent tubes to operate at the same pressure under all conditions.

Although the rear-slope surface pressures above the plenum-chamber slot became more positive for conditions of air flow through the slot (fig. 7), this variation in pressure was a local phenomenon and had a negligible effect on the vent-tube pressures.

The variation of vent-tube pressure with angle of attack for configuration E is also shown in figure 6. Satisfactory vent-tube pressures were obtained at all angles of attack investigated at a tunnel-air velocity of 250 feet per second (q_0, 13.1 in. water). Positive vent-tube pressures were obtained even at an angle of attack of -4°. No appreciable pressure variations among the vent tubes were observed. The vent-tube pressures obtained with configuration E for a given tunnel-air velocity and angle of attack were the highest for the configurations investigated.

Rain

In the simulated-rain condition, the vent ramp of configuration A was wetted by water runback on the airfoil surface; however, the water diverged ahead of the vent-tube openings and flowed into the corners at the rear slope of the configuration. From these areas, the water was observed to run back or blow off the surface. A 30-minute simulated rain period showed that no measurable amount of water was collected in the water trap.

Icing

Under normal flight conditions, the vent configurations investigated would not be subject to severe direct water impingement in an icing condition except at medium-to-high angles of attack. These conditions of attitude are usually encountered only during steep climb, low-speed cruise, or letdown and therefore occur for only a relatively short time interval. Because these icing investigations were conducted at very high angles of attack, at large liquid-water concentrations, and for long icing periods, the vent configurations were subjected to more severe icing conditions than would normally be encountered in flight.

Typical results of the icing investigations for configurations A to E are presented in figures 8 to 19, which include photographs of typical ice formations on the various configurations and plots of vent-tube pressure losses as a function of time in an icing condition.

In general, the icing investigations showed that the ice on the wing surface upstream of the vent ramp had a greater and more rapid effect on vent-tube pressure losses than icing of the vent configuration. These pressure losses were caused by the increased boundary-layer thickness over the wing resulting from the ice formations. Small but rough ice formations on the wing surface, especially at the start of an icing period, caused a greater vent-tube pressure loss than large ice ridges just aft of the heated leading edge. The effect of various protuberances on the airfoil surface upstream of the vent ramp is discussed in the appendix and correlated with observations made during the icing investigations.

Negative vent-tube pressures were realized in some instances for both cloud-icing and simulated freezing-rain conditions. For the configuration having the highest vent-tube pressure characteristics, negative pressure values were obtained only at low angles of attack in a freezing-rain condition. Because vent-tube air flows of the order of 0.5 pound per minute may occur during rapid descent and this condition is more conducive to vent-tube icing than a condition of no vent air flow, the air-flow inducing system shown in figure 4 was used throughout the icing investigations. Vent-tube air-flow losses amounting to 22 percent of the original air flow were observed. These air-flow losses, however, are considered excessive and not representative of actual flight air-flow losses because the change in pressure altitude, which induces vent-tube air flows during descent in flight, could not be duplicated in the tunnel investigations. The two methods of inducing air flow through the vent tubes are therefore inherently different and the results are not comparable.

Configuration A. - In configuration A, the vent lines remained relatively free of ice formations, although the vent-tube pressure decreased rapidly with time during the icing period. The vent ramp was severely iced only at the upstream end, and considerable ice formation accreted to the rear slope of the recess from a point above the tubes to the wing surface. The chamfered plate representing an actual wing-skin installation contributed only slightly to the growth of ice formations at the rear of the configuration. Ice formations in the vent tubes started to build up as frost formations on the downstream side of the tubes because this area is more susceptible to the direct impingement of very small water droplets. For long icing periods, 30 minutes or more, the entire inside of the vent tubes was coated with a very light ice formation that extended approximately 3 diameters into the tubes.

1053

Photographs of the typical progressive formation of ice on configuration A are shown in figure 8 for a 62-minute icing period. At the end of 15 minutes (fig. 8(a)), only a light ice formation was observed on the vent ramp and frost formations were present in the vent tubes. On the rear slope of the recess, a ridge of ice approximately 1/2 inch thick was built up near the wing surface. The reduction in the vent-tube diameters due to icing was small. The leading edge of the airfoil section was unheated for the first 15 minutes of the icing period. For the remainder of the icing period the leading edge was heated to 10 percent of chord.

Occasionally the growth of ice at the rear of the vent installation protruded into the air stream to such an extent that an ice scoop was obtained, as shown in figure 8(b). The increase in vent-tube pressure (fig. 9) in tube 1 during the 15- to 30-minute icing interval was a result of the scooping effect by the ice formations. When the ice scoop was blown off the surface, a sharp reduction in vent-tube pressure was observed.

Because scooping the air into the vent tubes by the ice formations improved the vent-tube pressures, additional experiments on configuration A were made using a sheet-metal ram scoop extending upstream of the rear slope of the recess to a point 1/4 inch forward of the vent-tube openings. This scoop was raised by increments from an initial flush position on the lower airfoil surface to a maximum of 3/8 inch above that surface. The results from these investigations showed that the ram scoops utilized did not extend far enough into the air stream to improve the vent-tube pressure characteristics of the configuration. A further increase in the scoop height above the surface was considered to be detrimental to the icing characteristics of the vent configuration because of the nature of exposed-scoop icing characteristics.

For the cloud-icing conditions investigated, static pressures in the vent tubes were reduced with progressive icing. The variation of vent-tube pressure with time for the icing conditions given for figure 8 is presented in figure 9. The vent-tube pressure differential p_s-p_0 is shown plotted as $\frac{p_s-p_0}{(p_s-p_0)_0}$ for a variation with time in an icing condition, where $(p_s-p_0)_0$ is the initial vent-tube pressure at the beginning of the icing period. It can be determined from figure 9 that at a tunnel velocity of 230 feet per second and an angle of attack of 16° (q_0, 12.8 in. water), the marginal vent-tube pressure was reached after 9 to 10 minutes in an icing condition. The vent-tube pressure-loss data presented herein are valid for the conditions investigated but may not necessarily be extrapolated for other icing conditions.

1033

During periods of tunnel shutdown to obtain photographs of ice formations on the model, the tunnel-air temperature rose and some of the ice formations on the model surfaces were blown off when the tunnel was restarted. As a result of the decreased ice formations on the surfaces, the vent-tube pressures increased after periods of shutdown (fig. 9).

In a simulated freezing-rain condition, the vent-tube pressure losses occurred more rapidly than during a cloud-icing condition. The ice formations on the airfoil were observed to build up normal to the surface rather than facing into the air stream and were consequently more severe than the formation observed for the icing conditions.

Configuration B. - In general, the cloud-icing investigation of configuration B showed that the vent lines remained ice-free, although the vent-tube pressures in the tubes were reduced. Considerable ice formations accreted to the rear slope of the vent installation and for long icing periods very light frost formations were observed in the vent tubes.

Photographs of typical formations of ice on configuration B are shown in figure 10 for a 60-minute icing period. At the end of an icing period of 30 minutes (fig. 10(a)), only a light ice formation was observed on the vent ramp, no ice nor frost was observed in the vent tubes, and the maximum ice thickness on the rear slope of the recess was 3/4 inch.

A scoop caused by the protrusion of ice formations into the air stream, as shown in figure 10(b), increased the vent-tube pressure in tube 4.

The variation of vent-tube pressures with time for the cloud-icing condition given for figure 10 is presented in figure 11. In general, the vent-tube pressure decreased rapidly with time during the icing period. As determined from figure 11, at a tunnel-air velocity of 230 feet per second (q_0, 12.7 in. water), the marginal vent-tube pressure was reached after 3 minutes in the icing condition.

Icing experiments were also conducted with configuration B at an angle of attack of 8°, a tunnel-air velocity of 400 feet per second, and at an ambient-air temperature of 20° F. Vent-tube marginal pressures at this velocity were reached after approximately 9 minutes in an icing condition having a liquid-water content of 1.0 gram per cubic meter.

1033

During the simulated freezing-rain experiment (fig. 12), the ice formation aft of the airfoil heater accreted normal to the surface to a maximum thickness of 2.5 inches. These heavy ice formations caused the vent-tube pressure to decrease with time at approximately twice the rate observed for the cloud-icing condition given for figure 10.

Configuration C. - Typical ice formations on configuration C are shown for 15- and 45-minute cloud-icing periods in figure 13. The general icing characteristics for this configuration were similar to, but more severe than, those observed for configuration B. In addition, an area reduction of the vent-tube openings resulting from icing was incurred.

The variation of vent-tube pressure with time for configuration C during the 45-minute icing period is shown in figure 14. The marginal vent-tube pressure for the outer tubes at a tunnel-air velocity of 230 feet per second (q_0, 13.3 in. water) was reached after 15 minutes in the icing condition, as can be determined from figure 14. Without scooping caused by ice formations, the inner vent tubes reach the marginal pressure after 10 minutes of icing. A high vent-tube pressure was maintained by tube 2 throughout the icing period because of the scooping caused by the ice formation shown in figure 13. A smaller ice scoop above tube 3 maintained a positive though submarginal pressure in this tube throughout the icing period.

Configuration D. - The cloud-icing characteristics of configuration D were similar to those of configuration C and more severe than those observed for configuration A. Typical ice formations on configuration D are shown in figure 15 for 30- and 60-minute cloud-icing periods.

The usual protrusion of the ice formations into the air stream above the vent-tube openings are shown in figure 15(a). The resulting scooping effect by these ice formations maintained or increased the vent-tube pressure in the inner vent tubes until the ice scoops were removed from the surface by blow-off. At the end of the 60-minute icing period (fig. 15(b)), the area of the large-diameter vent tubes was approximately halved whereas the area of the small vent tube was reduced to approximately one-twentieth of the original area.

The variation of vent-tube pressures with time in a cloud-icing period for configuration D is shown in figure 16. Because the vent-tube pressures at the start of an icing period for this configuration

1033

were considerably greater than those of the three previous configurations investigated, the time required to reduce the vent-tube pressures to the marginal value in an icing condition was increased to 17 minutes, as can be determined from figure 16. The scooping effect of ice formations at the rear slope of the recess above the inner vent tubes caused the increase in vent-tube pressures shown for vent tubes 2 and 3 in figure 16. The removal of the ice scoop by blow-off after 40 minutes in the icing condition caused an immediate decrease in vent-tube pressure for tubes 2 and 3.

Vent configuration D was also investigated at a tunnel-air velocity of 400 feet per second and at an angle of attack of 8° for a 30-minute icing period under the following cloud-icing conditions: ambient-air temperature, 20° F; and liquid-water content, 1.0 gram per cubic meter. The results showed that the icing characteristics were similar to those observed at the lower air velocity and higher angle of attack. The vent-tube pressures remained greater than the marginal requirement throughout the icing period.

In a simulated freezing-rain condition at a tunnel-air velocity of 220 feet per second and at an angle of attack of 14°, the vent-tube pressures for configuration D decreased more rapidly than during a cloud-icing condition. The marginal vent-tube pressures in the outer tubes were reached after 7.5 minutes, whereas the pressures in the inner tubes were marginal after approximately 12 minutes.

Configuration E. - Typical ice formations on configuration E are shown in figure 17 for a 60-minute cloud-icing period. Ice formations on the rear slope of the vent above the plenum-chamber slot (fig. 17(a)) formed a large scoop, which helped to maintain a high vent-tube pressure throughout the remainder of the icing period. At the end of the 60-minute icing period, the plenum-chamber-slot area was reduced to approximately 35 percent of the original area.

The variation of vent-tube pressures with time for the cloud-icing condition given in figure 17 is shown in figure 18. During the first 10 minutes of the icing period, the vent-tube pressure-differential ratio decreased rapidly to a value of 0.56; for the remainder of the icing period, this pressure ratio ranged from 0.43 to 0.63. At no time for this icing condition did the vent-tube pressures for configuration E decrease to the marginal-pressure value. The large reduction in plenum-chamber-slot area did not appear to affect seriously the pressure in the vent tubes.

Cloud-icing investigations were also conducted with configuration E at tunnel-air velocities of 375 and 470 feet per second at angles of attack of 8° and 3.6°, respectively, for an average liquid-water content of 0.6 gram per cubic meter at an ambient-air temperature of 22° F. The results showed that the initial decrease in vent-tube pressure-differential ratio was greater than that shown in figure 18; however, the vent-tube pressure differentials were greater than the marginal requirements throughout the 10-minute icing period.

Cloud-icing investigations conducted at an ambient-air temperature of 0° F resulted in approximately the same reduction in vent-tube pressure-differential ratios as those observed at the higher ambient-air temperatures.

In a simulated freezing-rain condition, the vent-tube pressures decreased more rapidly than during a cloud-icing condition, as shown in figure 19. The marginal vent-tube pressures at an angle of attack of approximately 14° and a tunnel-air velocity of 220 feet per second were reached after $7\frac{1}{2}$ minutes; whereas, at an angle of attack of 3.6° and a tunnel-air velocity of 400 feet per second, the marginal pressure was reached after $2\frac{1}{4}$ minutes (fig. 19). At an angle of attack of 3.6°, negative vent-tube pressures were observed after 5 minutes.

Effect of leading-edge heating on vent-tube pressure characteristics in cloud-icing conditions. - Investigations were made with configuration E to determine the effect of leading-edge heating on the vent-tube pressure losses in a cloud-icing condition. The experiments were made without heat and with heat applied to 5-, 10-, and 20-percent chord under the same icing conditions. The results showed that use of heat produced the same rapid decrease in vent-tube pressure with 5-, 10-, or 20-percent chord. For an unheated leading edge, the initial decrease in vent-tube pressures was considerably less than that observed with leading-edge heating. At the end of 20 minutes, the vent-tube pressure ratios were approximately the same for unheated and all heated leading-edge conditions. The more rapid vent-tube pressure losses with leading-edge heating were caused by refreezing of water runback ahead of the vent ramp as well as large ridges of ice aft of the heated area.

SUMMARY OF RESULTS

From an aerodynamic and icing investigation conducted in the NACA Lewis icing research tunnel on several recessed fuel-vent configurations, the following results were obtained:

Aerodynamic

1. Configurations with diverging ramp sidewalls maintained vent-tube pressures greater than the marginal positive pressure-differential requirement of 2 inches of water between the fuel cell and the compartment containing the fuel cell for a range of angles of attack from 0° to approximately 14° at a tunnel-air velocity of approximately 240 feet per second. Configurations with parallel ramp walls showed submarginal vent-tube pressure characteristics at angles of attack less than 4° and 6° at the same tunnel-air velocity.

2. The configurations utilizing individual vent-tube openings and diverging ramp walls showed a marked decrease in vent-tube pressures in the outer tubes.

3. The configuration having diverging ramp sidewalls, a 7° ramp angle, and vent tubes manifolded to a common plenum chamber opening through a slot in the ramp floor gave the highest vent-tube pressures for all angles of attack and tunnel-air velocities investigated. The use of the plenum chamber resulted in uniform pressures in all vent tubes under all conditions investigated.

Icing

4. Rapid losses in vent-tube pressures during the first few minutes in icing conditions were caused by the roughness of the ice formations on the airfoil surface ahead of the vent ramp rather than by the icing of the vent configuration.

5. In similar cloud-icing conditions, only the configuration in which the highest vent-tube pressures were attained maintained the required vent-tube pressure throughout a 60-minute icing period. In general, the configurations with diverging ramp walls maintained adequate vent-tube pressures for a longer period of time in an icing condition than configurations with parallel ramp walls.

6. For similar cloud-icing conditions, the ice formations on the rear wall slope for configurations with diverging ramp walls were more severe than those observed for configurations with parallel walls. These more severe ice formations, however, did not appreciably influence the vent-tube pressures.

7. At an angle of attack of 14° and at a tunnel-air velocity of 240 feet per second, no complete closure of vent-tube openings due to ice formations occurred for the configurations investigated, although the areas of the vent-tube openings and the plenum-chamber entrance were considerably reduced in some instances by ice formations.

8. For simulated freezing-rain conditions, the vent-tube pressure losses for all configurations were greater and occurred more rapidly than those observed for a cloud-icing condition. These large and rapid vent-tube pressure losses were more detrimental at the smaller angles of attack because the marginal pressure values were reached in a matter of minutes.

9. Negative vent-tube pressures were realized in some instances for both cloud-icing and simulated freezing-rain conditions. For the configuration having the highest vent-tube pressure characteristics, negative pressure values were obtained only at low angles of attack in a freezing-rain condition.

DESIGN RECOMMENDATIONS

On the basis of the results obtained from this investigation of recessed fuel-vent configurations, the following design recommendations can be made:

1. A recessed fuel-vent configuration having a ramp angle of 7°, diverging ramp sidewalls, and vent tubes manifolded to a slot opening in the ramp floor at the point of maximum recess should be used to obtain the most satisfactory aerodynamic and icing characteristics.

2. A plenum chamber should be used between the slot opening in the ramp floor and the vent tubes in order to afford uniform vent-tube pressures under all operating conditions.

3. The ratio of slot width to maximum vent width should not exceed 0.55 because of the spanwise pressure gradient across the configuration.

4. No protuberances should be located on the surface ahead of the vent ramp.

Lewis Flight Propulsion Laboratory,
National Advisory Committee for Aeronautics,
Cleveland, Ohio, September 24, 1948.

1033

APPENDIX

EFFECT OF SURFACE PROTUBERANCES ON FUEL-VENT AERODYNAMIC CHARACTERISTICS

In order to determine the effect of various types of surface protuberance on the vent-tube and ramp-pressure characteristics, several investigations of roughness were made with configuration E. Varying degrees of roughness were obtained by use of abrasion paper ($3\frac{1}{2}$ - 20), semicircular rubber strips of $\frac{1}{4}$-inch radius and 2-inch lengths, and a $\frac{7}{8}$ by $1\frac{1}{4}$ by 12 inches sponge-rubber pad.

Results of the roughness investigations are presented in figure 20. The abrasion paper, which was cemented to the wing surface from 25-percent chord to 2 inches upstream of the vent ramp, caused a sharp decrease in vent-tube pressure similar to that which might be caused by ice formations accreting to the airfoil surface at the beginning of an icing period.

Abrasion paper cemented only on the vent-ramp surface caused less reduction in vent-tube pressures than the abrasion paper on the airfoil surface. These results were verified during the icing investigations by visual observations when no ice was detected on the vent ramp or in the vent tubes during the first few minutes of an icing period. During this time, the airfoil surface became coated with light ice formations and the vent-tube pressures decreased rapidly. When the airfoil was completely de-iced at the end of an icing period while the vent remained iced, a large increase in vent-tube pressure resulted.

Rubber strips cemented to the airfoil surface just ahead of the vent ramp caused the largest vent-tube pressure losses, which indicated that if ice ridges are allowed to form in this location, the vent-tube pressures will be considerably reduced. When the rubber strips were located at the 25-percent chord station, the vent-tube pressures approached the values obtained with a normal surface.

The results obtained with the rubber pad cemented to the airfoil surface at 21-percent of chord, representing heavy ice ridges behind the heated area, showed vent-tube pressure losses similar to those obtained with abrasion paper on the ramp surface. During the icing investigations with configuration E, when heavy ridges of ice aft of the heater were blown off, the remaining rough, but

1033

relatively fine-grain, surface ice ahead of the vent ramp caused a marked decrease in the vent-tube pressures. This observation is in agreement with the curves for the rubber pad and abrasion paper shown in figure 20 in that a fine-grain roughness causes a greater decrease in vent-tube pressure than a large single spanwise protuberance.

The icing and roughness investigations have established that surface icing or roughness ahead of the vent ramp has a much greater effect on vent-tube pressure reductions than icing or roughness of the vent itself.

REFERENCES

1. Theodorsen, Theodore, and Clay, William C.: The Prevention of Ice Formation on Gasoline Tank Vents. NACA TN No. 394, 1931.

2. Allen, H. Julian, and Vincenti, Walter G.: Wall Interference in a Two-Dimensional-Flow Wind Tunnel with Consideration of the Effect of Compressibility. NACA TR No. 782, 1944.

TABLE I - ORDINATES FOR DIVERGENT RAMP WALLS

OF FUEL-VENT CONFIGURATIONS C, D, AND E

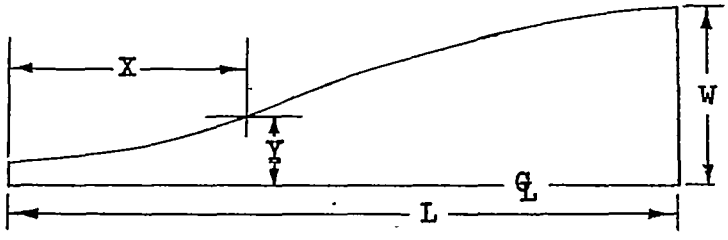

X/L	Y/W Configuration	
	C and D	E
0	0.130	0.084
.10	.160	.160
.20	.226	.236
.30	.318	.314
.40	.440	.390
.50	.581	.466
.60	.712	.614
.70	.823	.764
.80	.921	.914
.90	.986	.994
1.00	1.000	1.000

NACA

Figure 1. - Typical fuel-vent configuration mounted on NACA 65,2-216 airfoil section in test section of icing research tunnel.

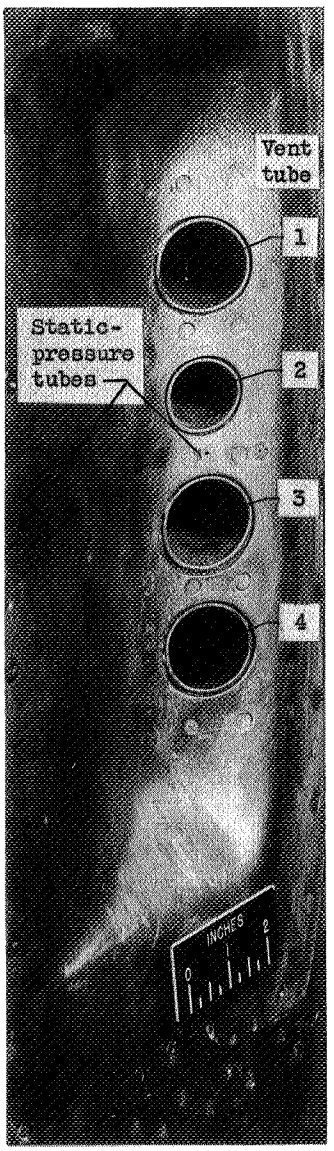

NACA
C-20426
1-16-48

(a) Configuration A.

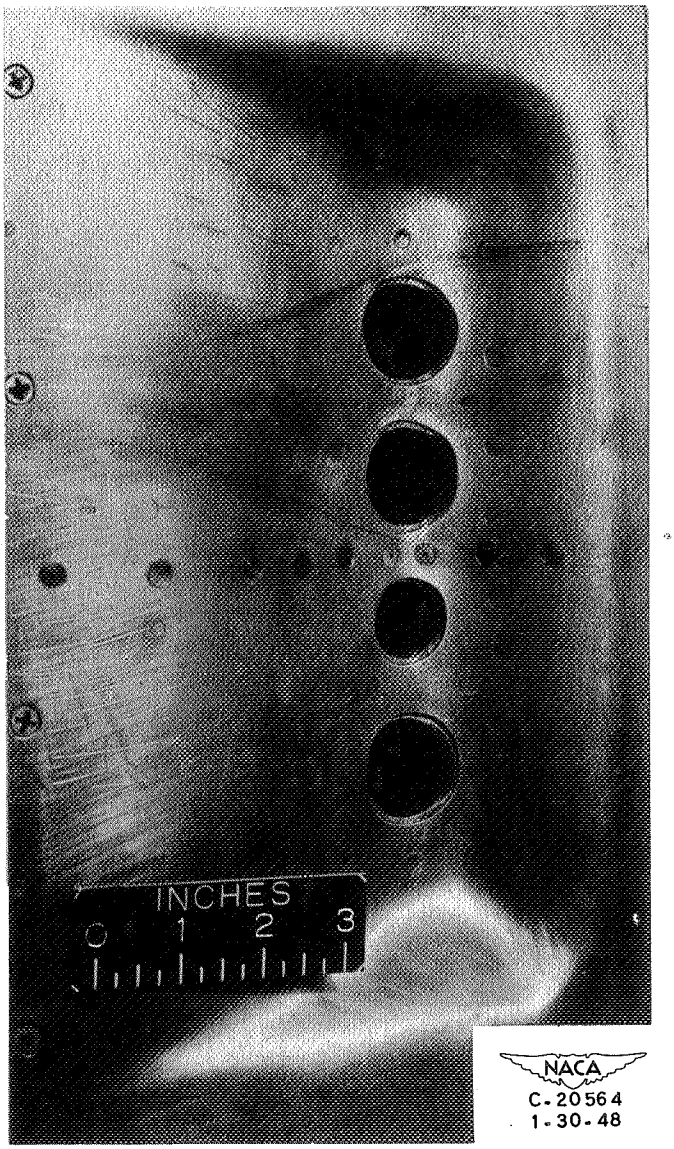

NACA
C-20564
1-30-48

(b) Configuration B.

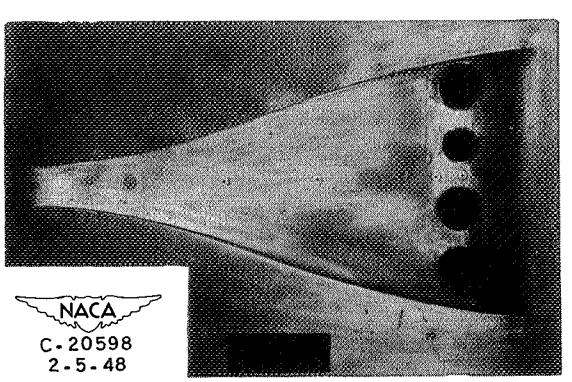

NACA
C-20598
2-5-48

(c) Configuration C.

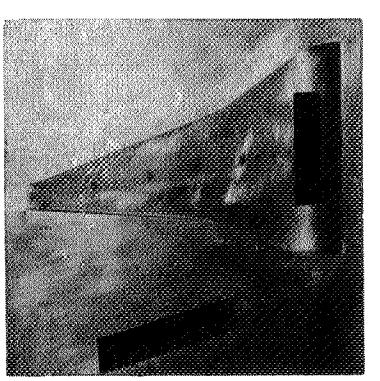

NACA
C-20988
3-30-48

(d) Configuration E.

Figure 2. - Close-up views of fuel-vent configurations.

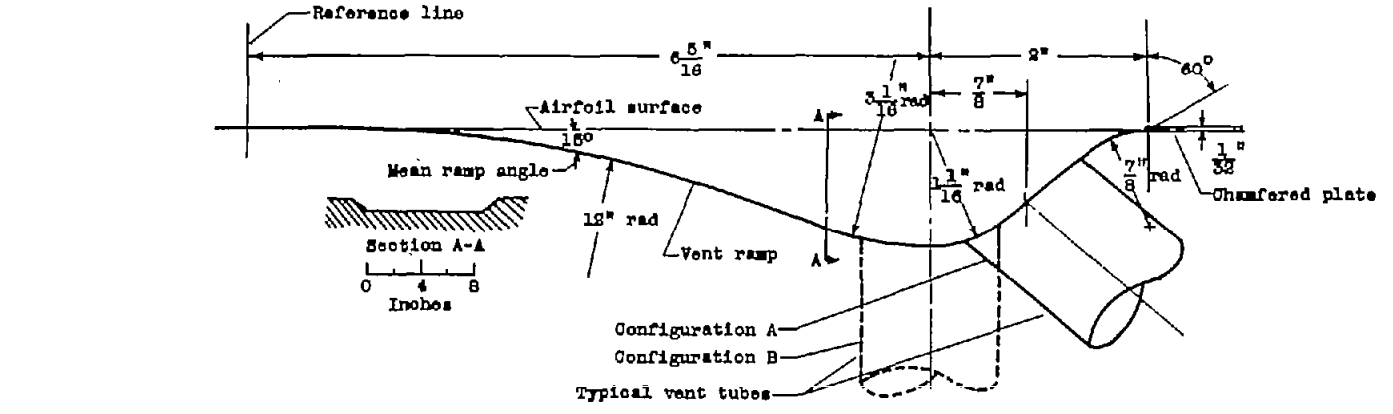

(a) Configurations A and B.

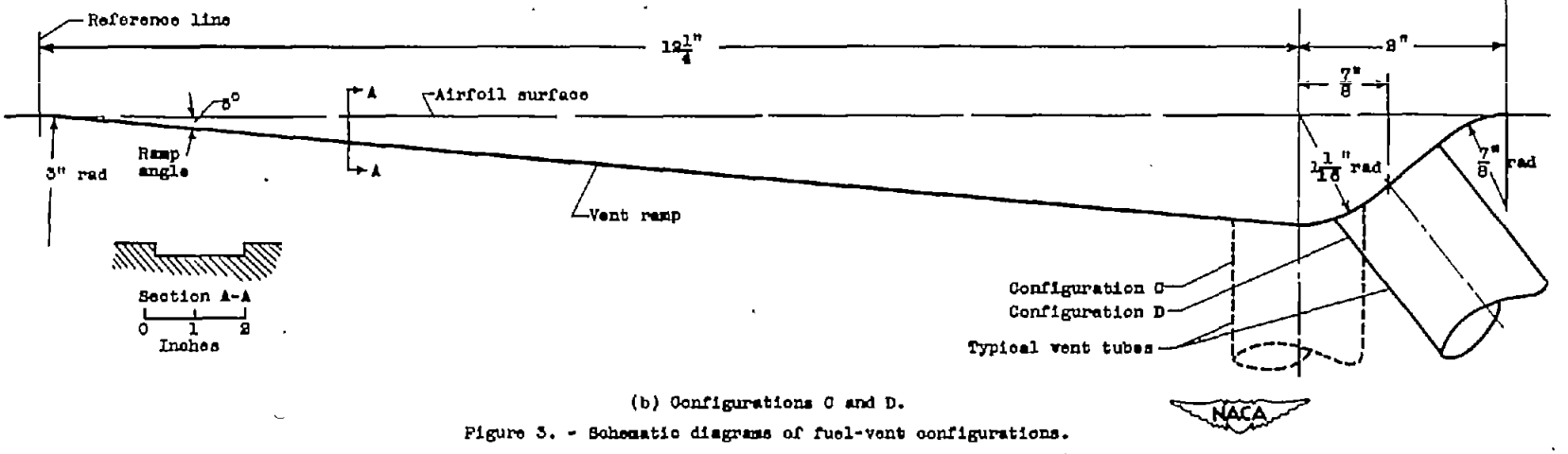

(b) Configurations C and D.

Figure 3. - Schematic diagrams of fuel-vent configurations.

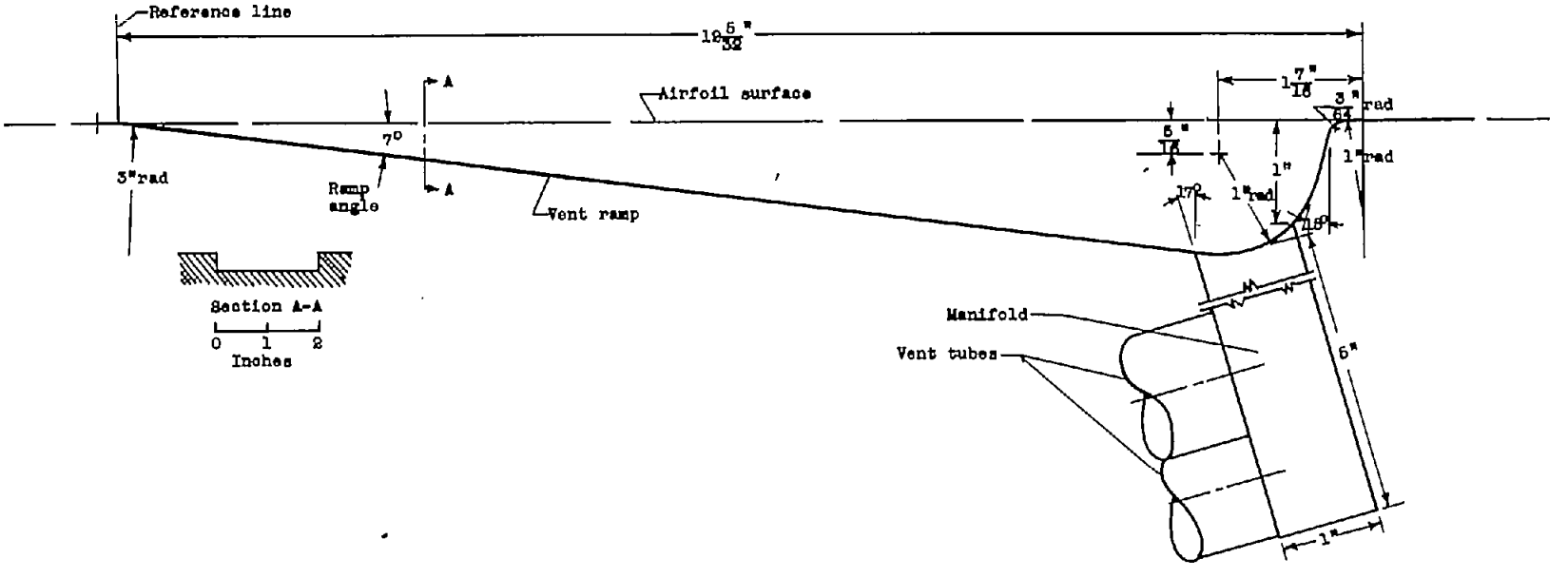

(c) Configuration E.

Figure 3. - Concluded. Schematic diagrams of fuel-vent configurations.

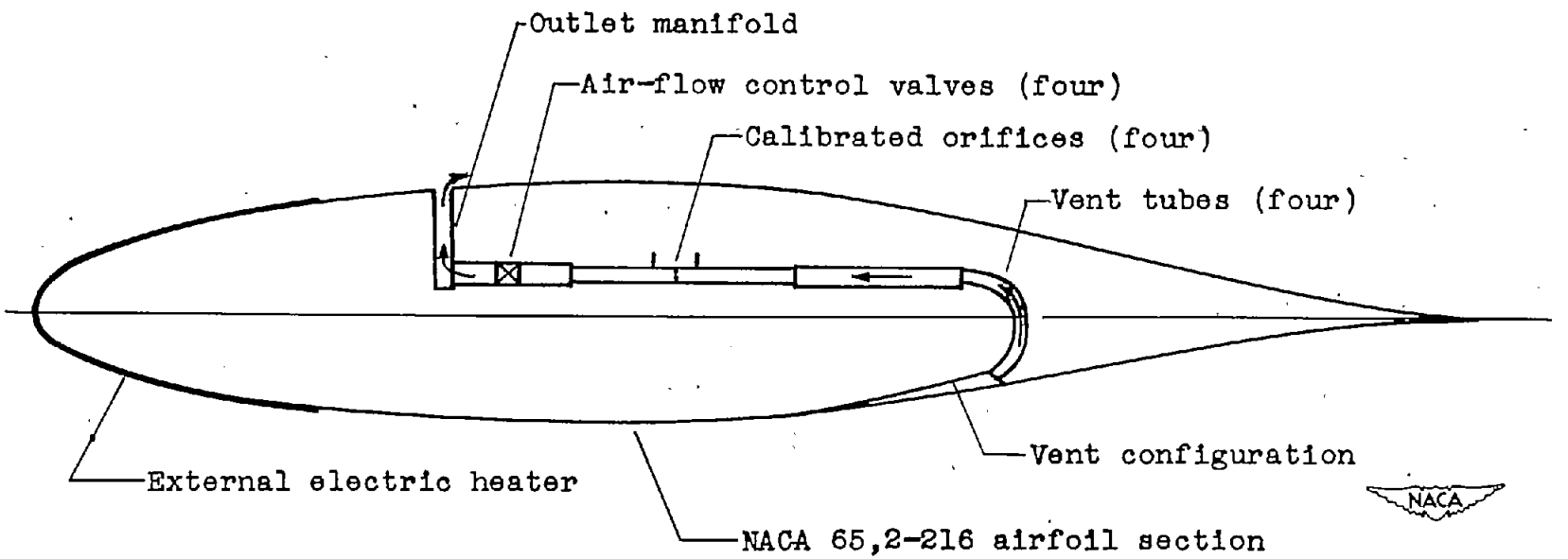

Figure 4. - Schematic diagram showing experimental set-up used in fuel-vent investigation.

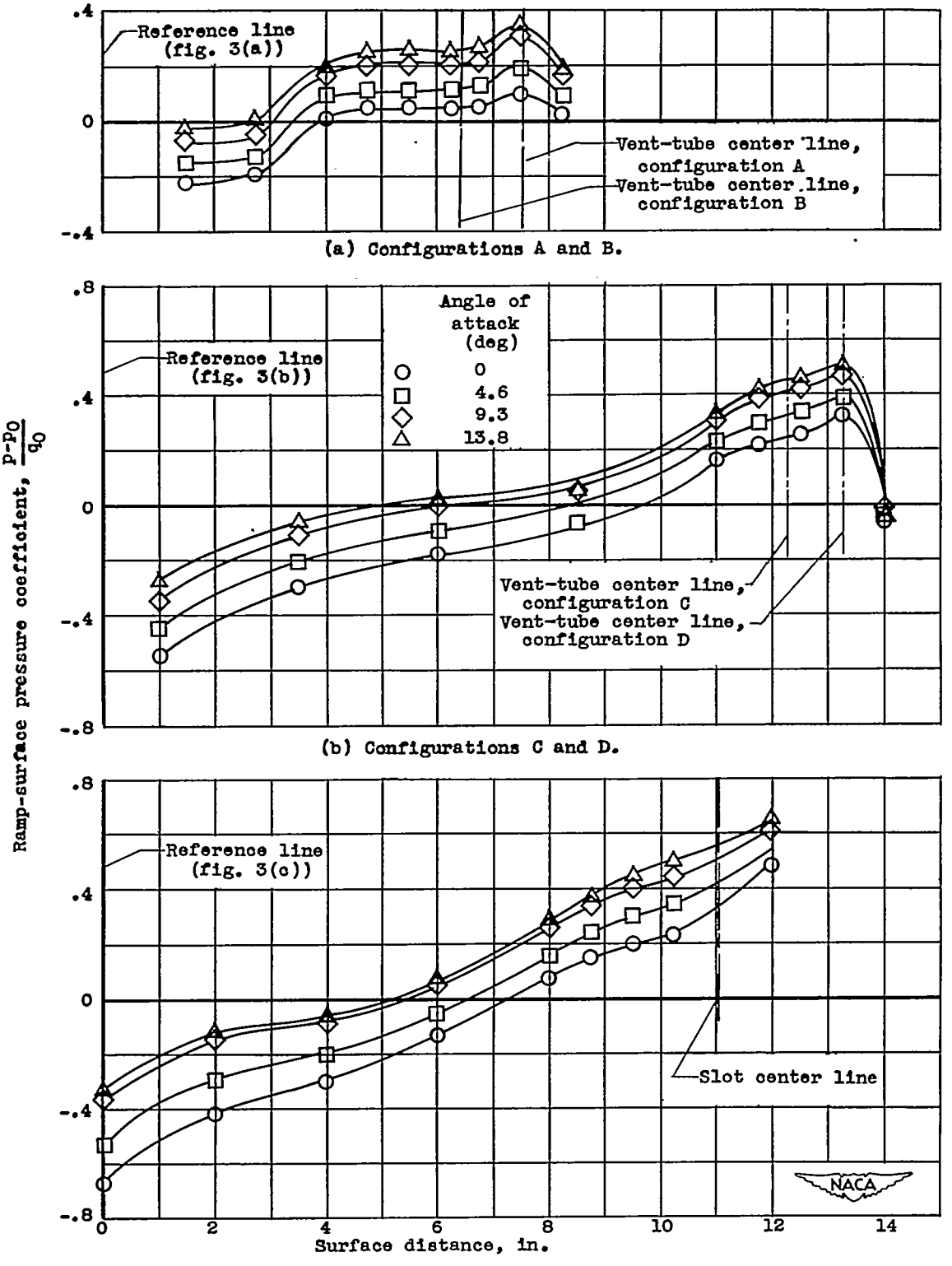

(a) Configurations A and B.

(b) Configurations C and D.

(c) Configuration E.

Figure 5. - Variation of ramp-surface-pressure distribution with angle of attack. No vent air flow.

1033

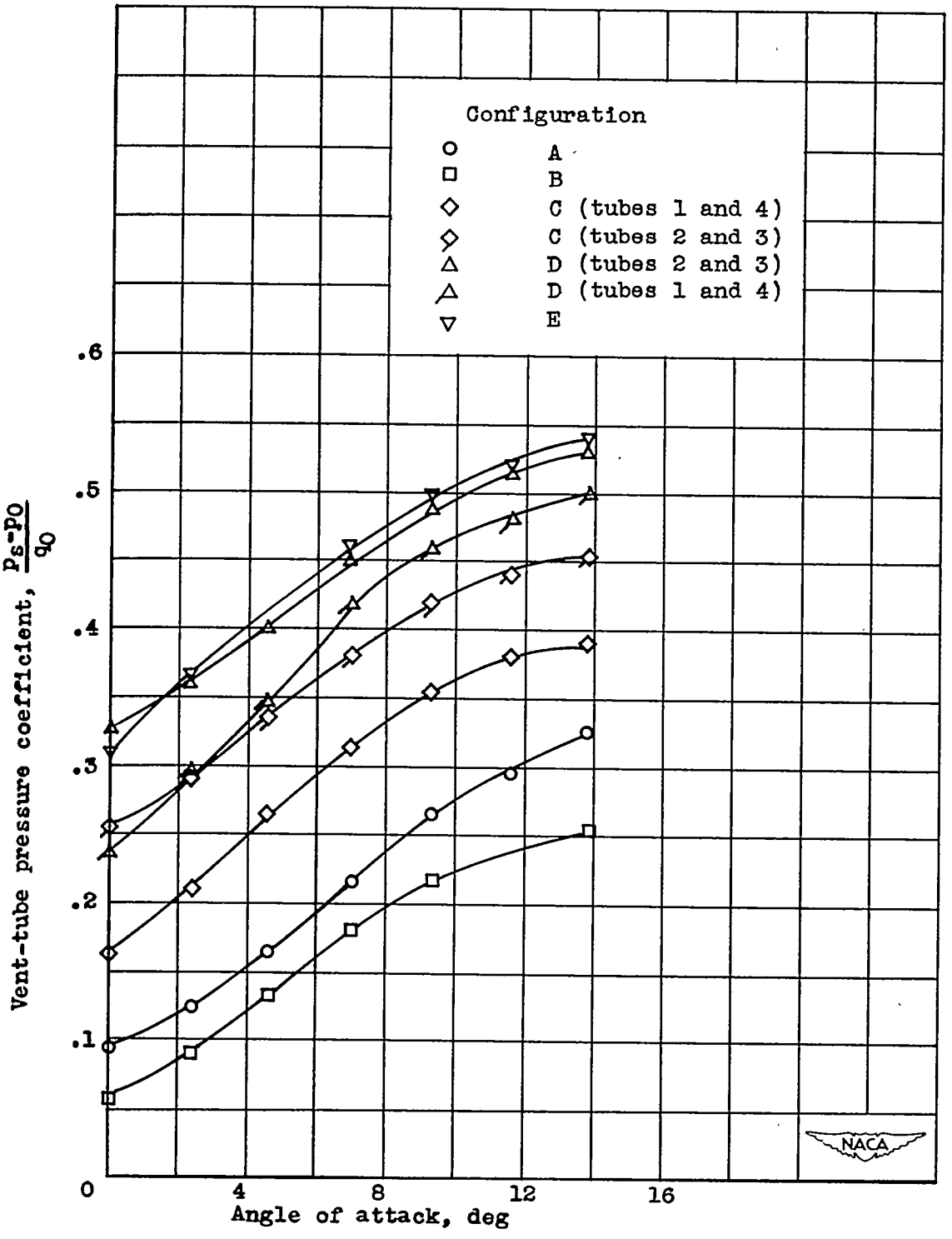

Figure 6. - Variation of average vent-tube pressure coefficient with angle of attack.

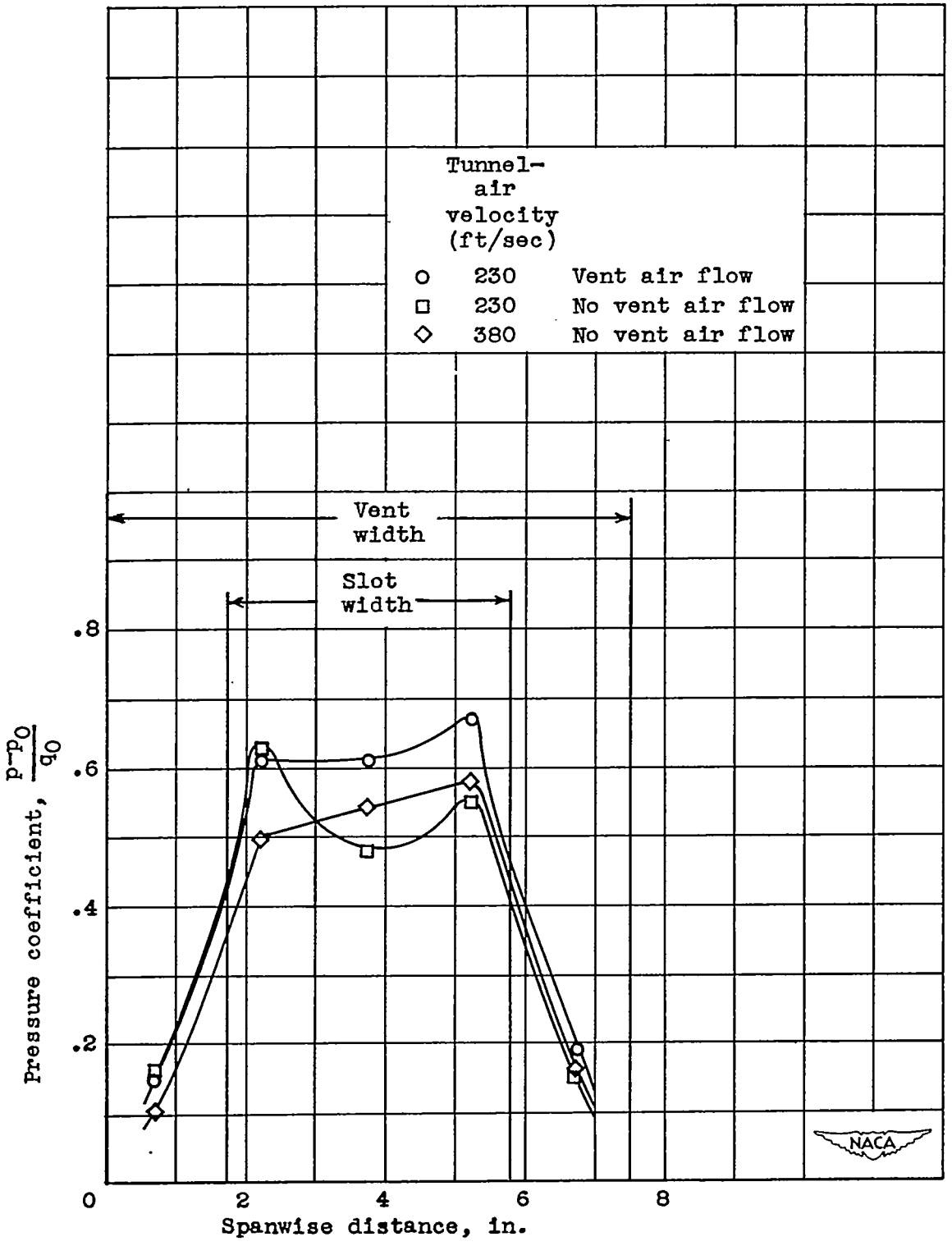

Figure 7. - Spanwise pressure distribution across rear slope of configuration E. Angle of attack, 0°.

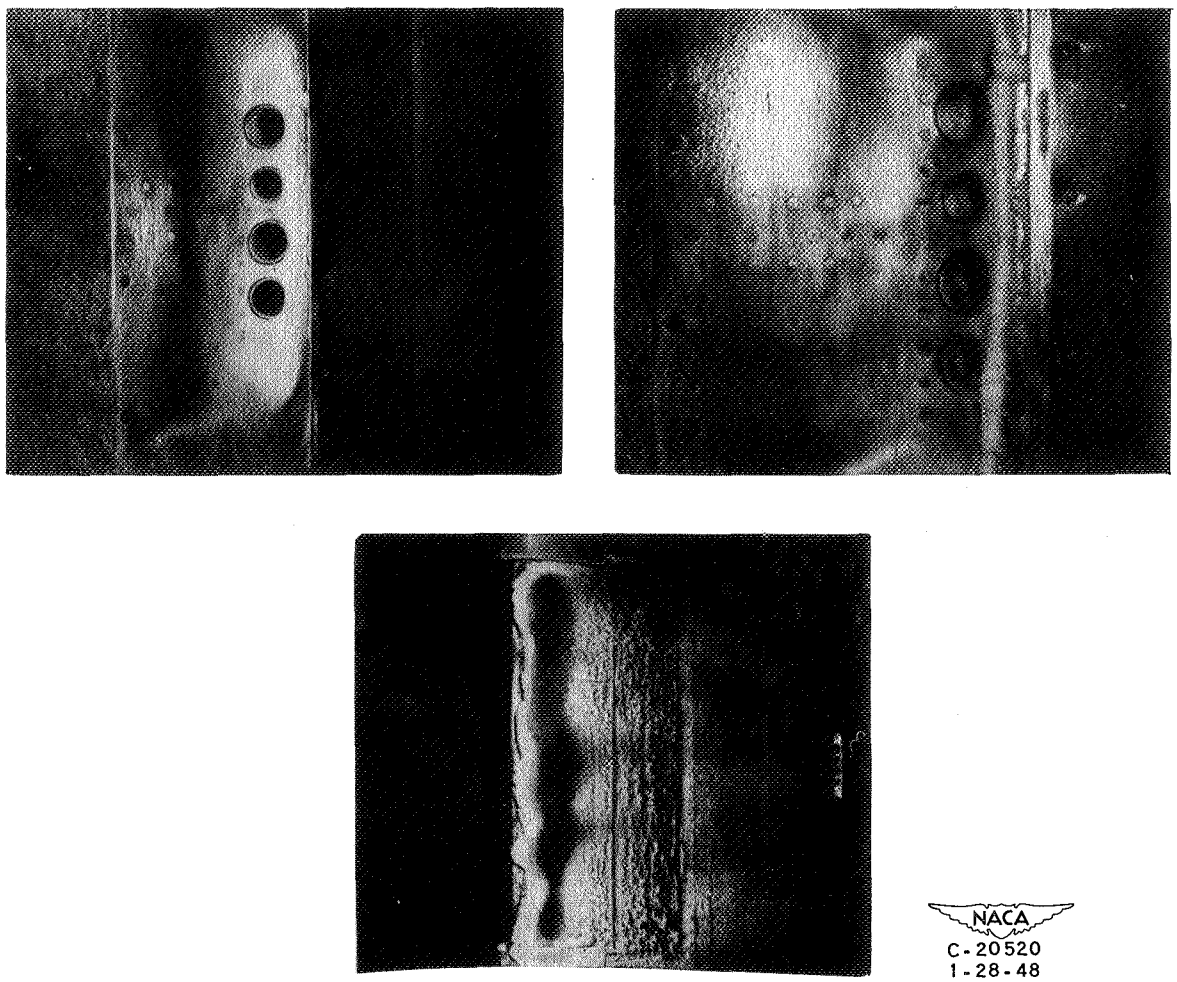

(a) Ice accretions following 15-minute icing period without leading-edge heating.

Figure 8. - Ice formations on airfoil surface and configuration A. Tunnel-air velocity, 230 feet per second; angle of attack, 16°; ambient-air temperature, 23° F; liquid-water content, 1.5 grams per cubic meter.

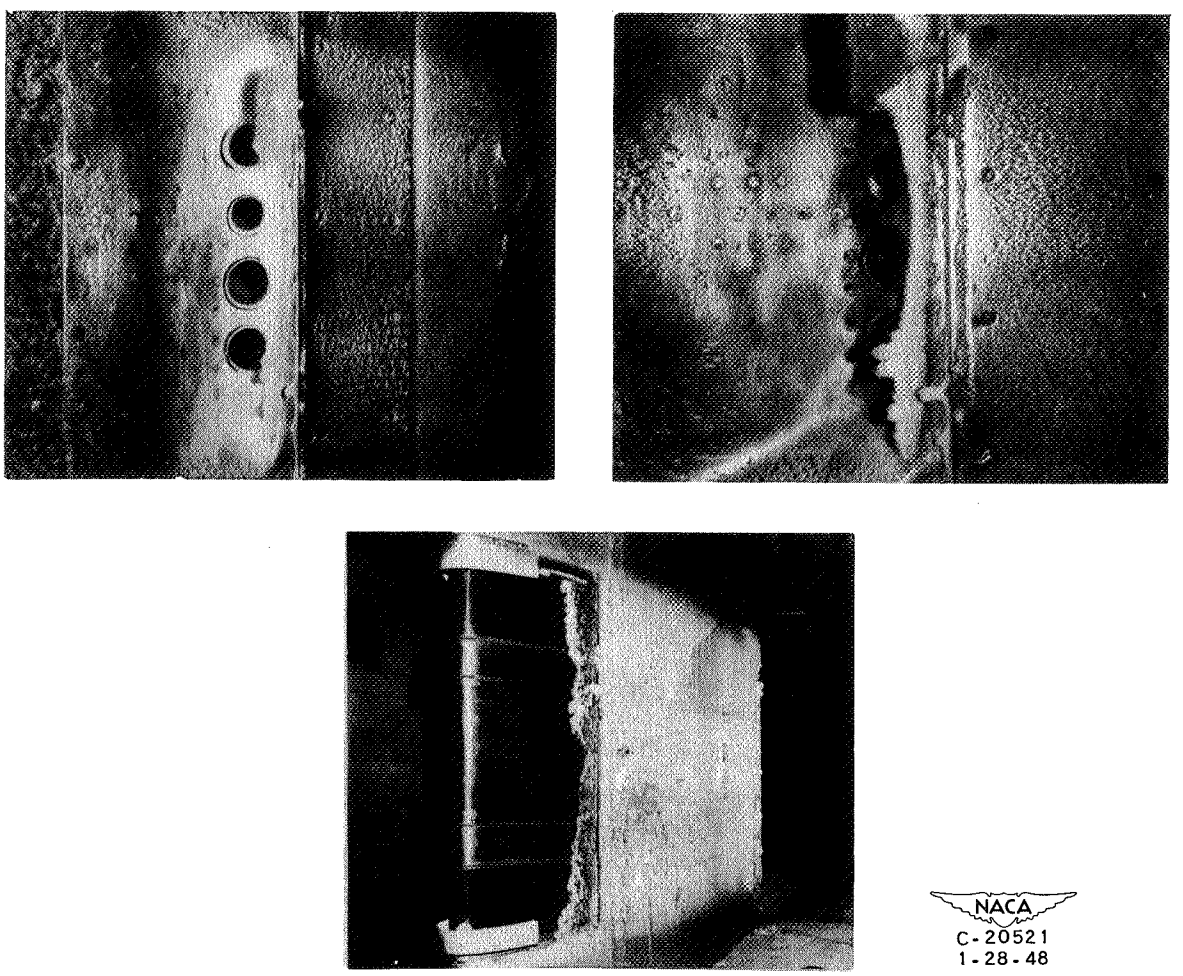

NACA
C-20521
1-28-48

(b) Ice accretions following 30-minute icing period with leading-edge heating.

Figure 8. - Continued. Ice formations on airfoil surface and configuration A. Tunnel-air velocity, 230 feet per second; angle of attack, 16°; ambient-air temperature, 23° F; liquid-water content, 1.5 grams per cubic meter.

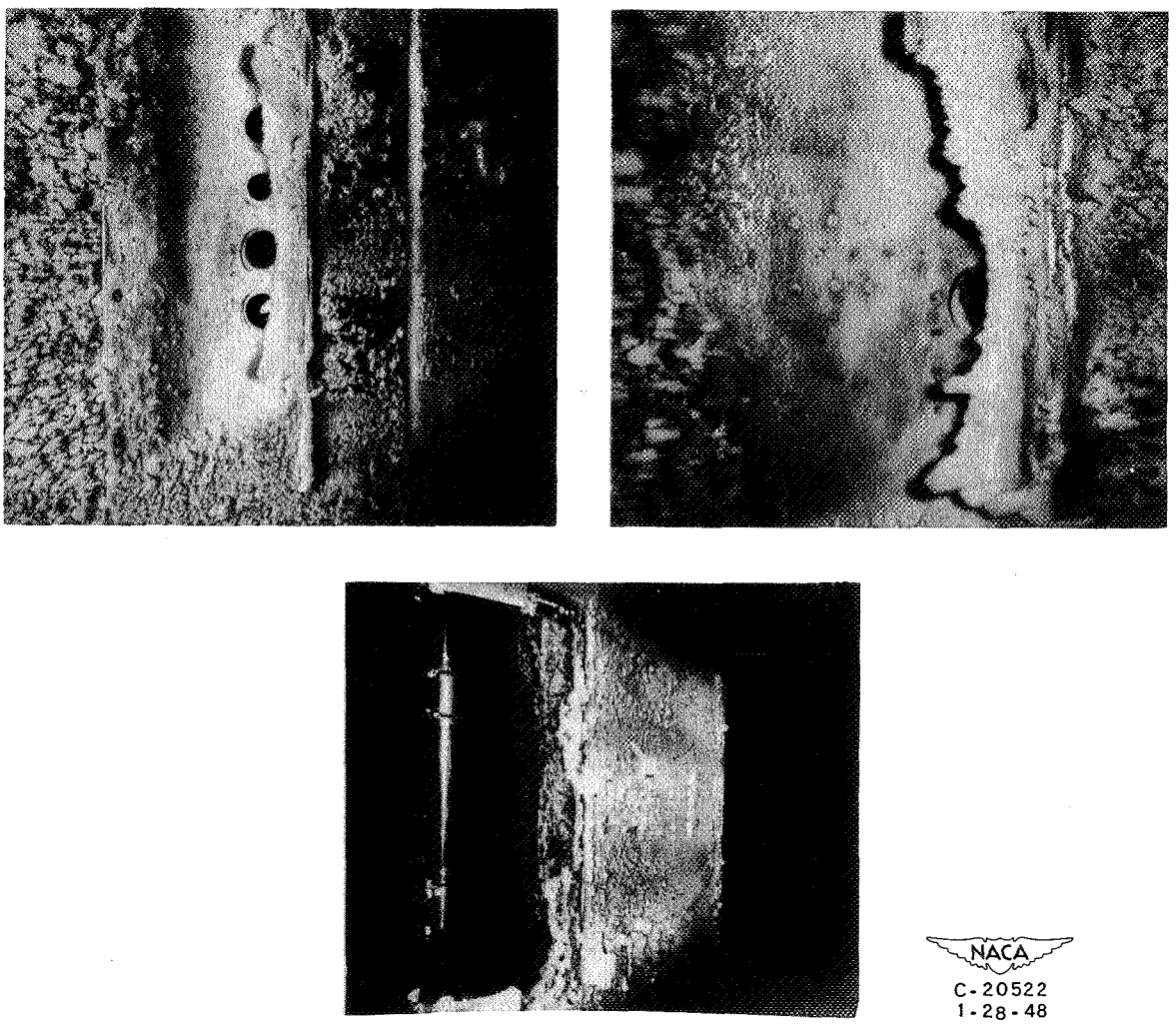

(c) Ice accretions following 62-minute icing period with leading-edge heating.

Figure 8. - Concluded. Ice formations on airfoil surface and configuration A. Tunnel-air velocity, 230 feet per second; angle of attack, 16°; ambient-air temperature, 23° F; liquid-water content, 1.5 grams per cubic meter.

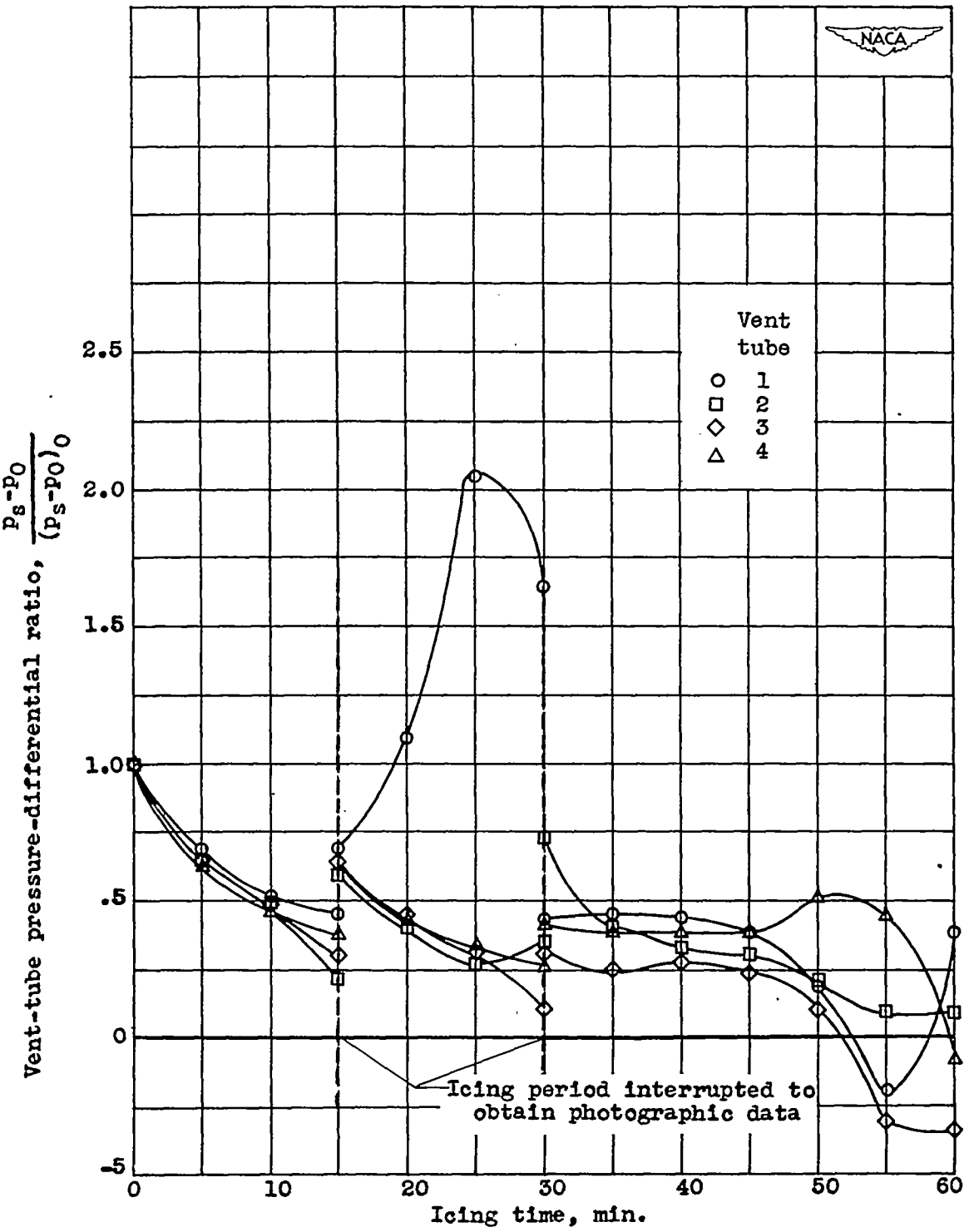

Figure 9. - Variation of vent-tube pressure differential with time for 62-minute icing period with configuration A. Average $(p_s-p_0)_0$, 3.9 inches water; tunnel-air velocity, 230 feet per second; angle of attack, 16°; ambient-air temperature, 23° F; liquid-water content, 1.5 grams per cubic meter.

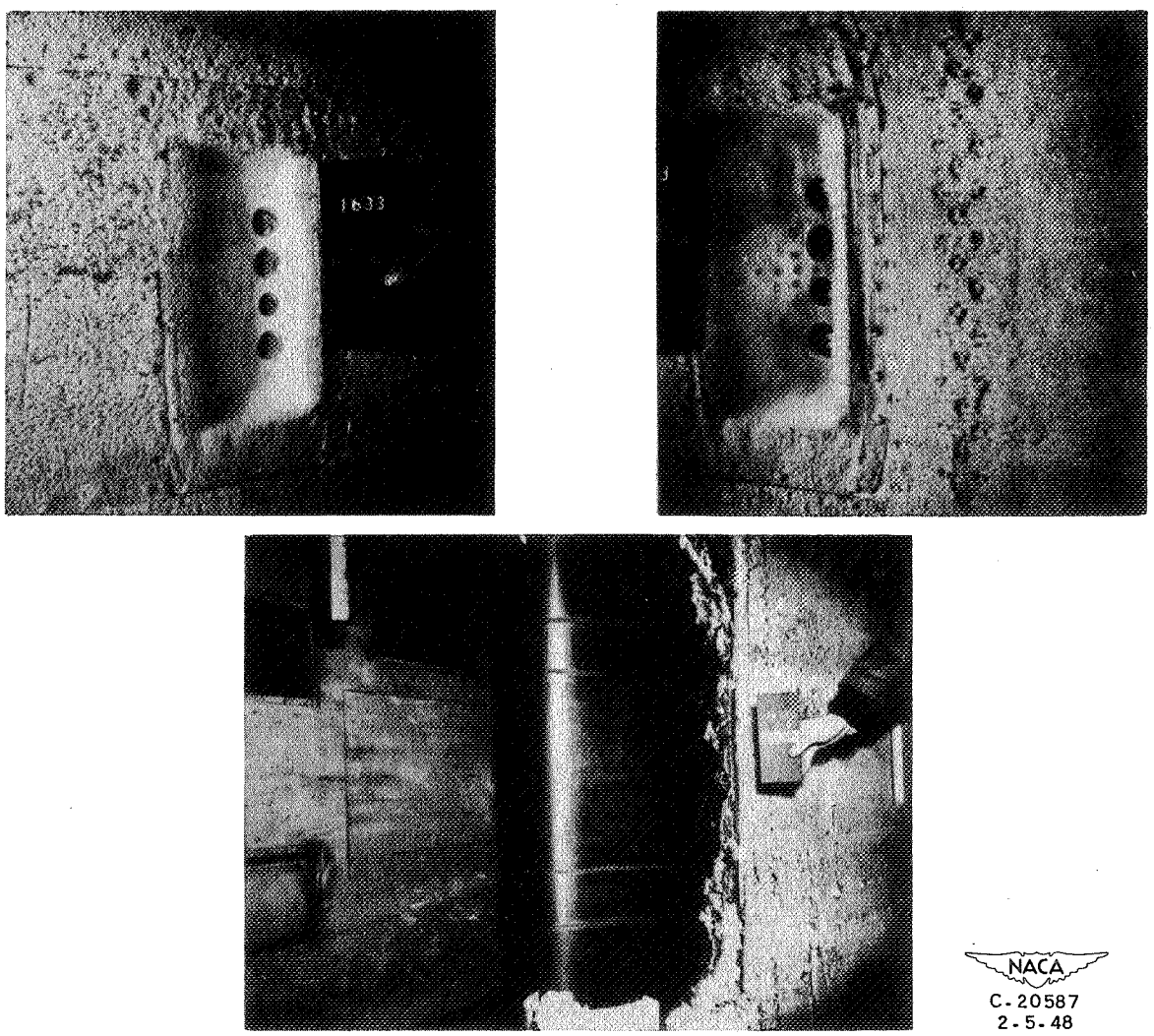

(a) Ice accretions following 30-minute icing period with leading-edge heating.

Figure 10. - Ice formations on airfoil surface and configuration B. Tunnel-air velocity, 230 feet per second; angle of attack, 16°; ambient-air temperature, 23° F; liquid-water content, 1.5 grams per cubic meter.

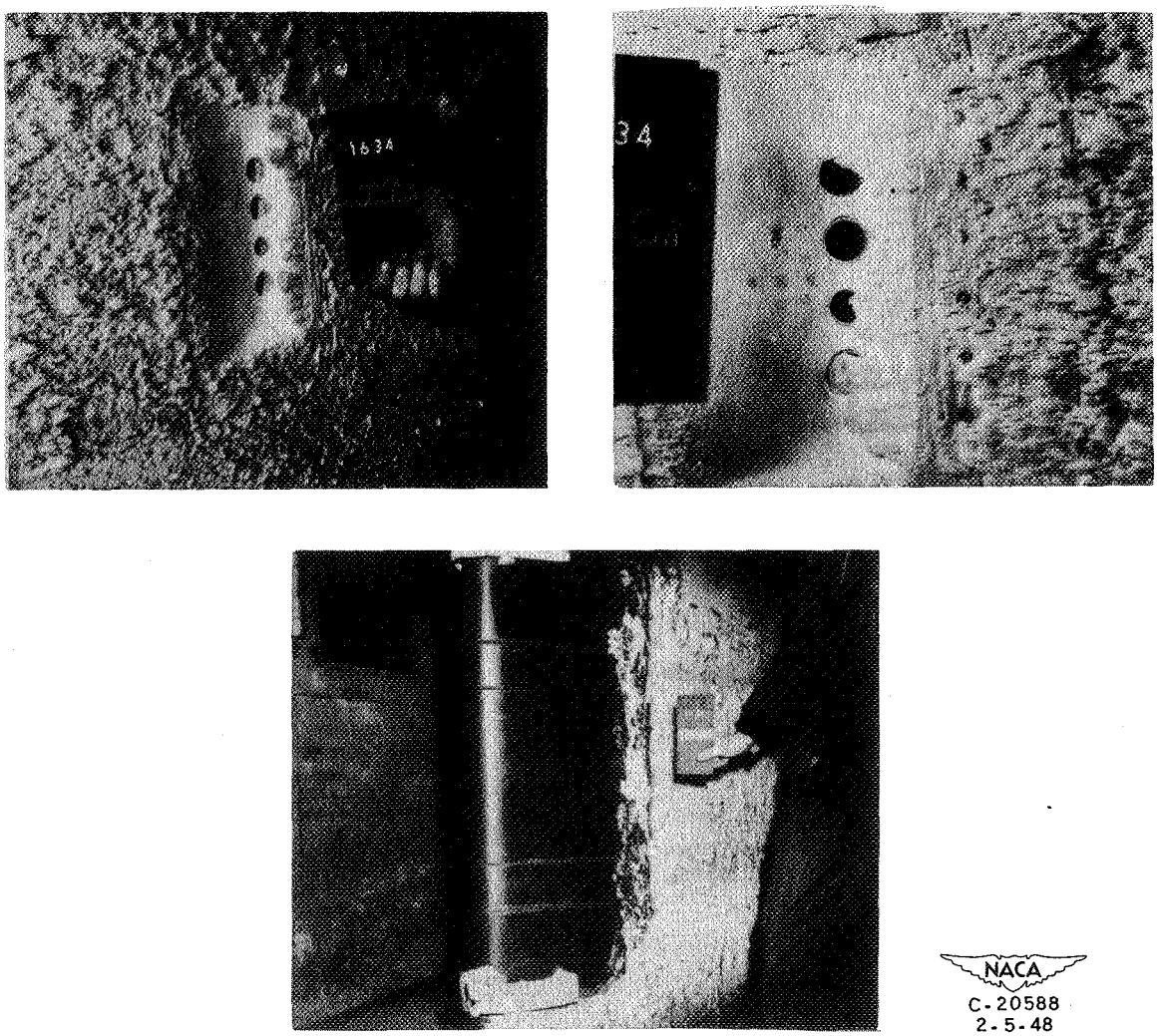

(b) Ice accretions following 60-minute icing period with leading-edge heating.

Figure 10. - Concluded. Ice formations on airfoil surface and configuration B. Tunnel-air velocity, 230 feet per second; angle of attack, 16°; ambient-air temperature, 23° F; liquid-water content, 1.5 grams per cubic meter.

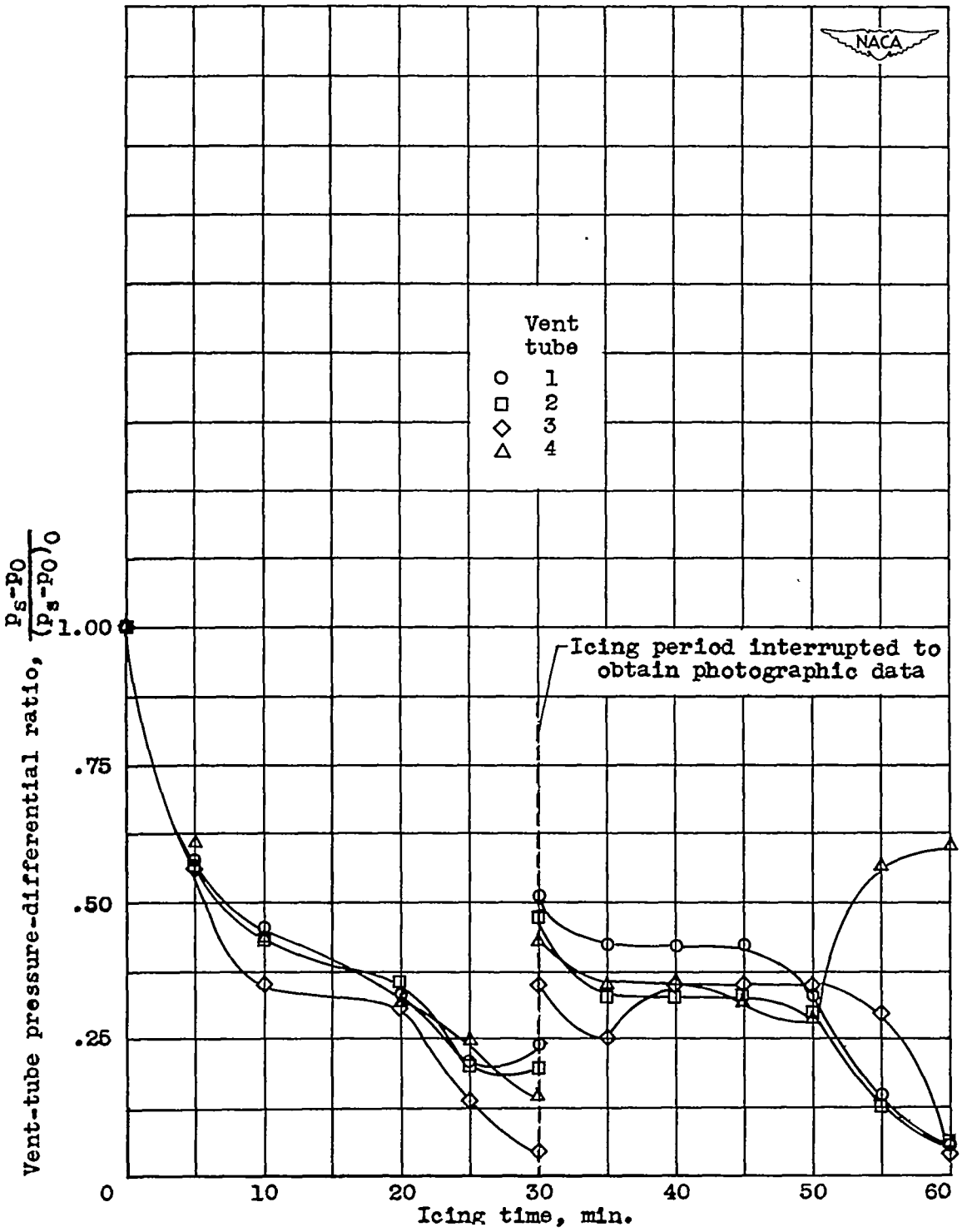

Figure 11. - Variation of vent-tube pressure differential with icing time for 60-minute icing period with configuration B. Average $(p_s-p_0)_0$, 2.9 inches water; tunnel-air velocity, 230 feet per second; angle of attack, 16°; ambient-air temperature, 23° F; liquid-water content, 1.5 grams per cubic meter.

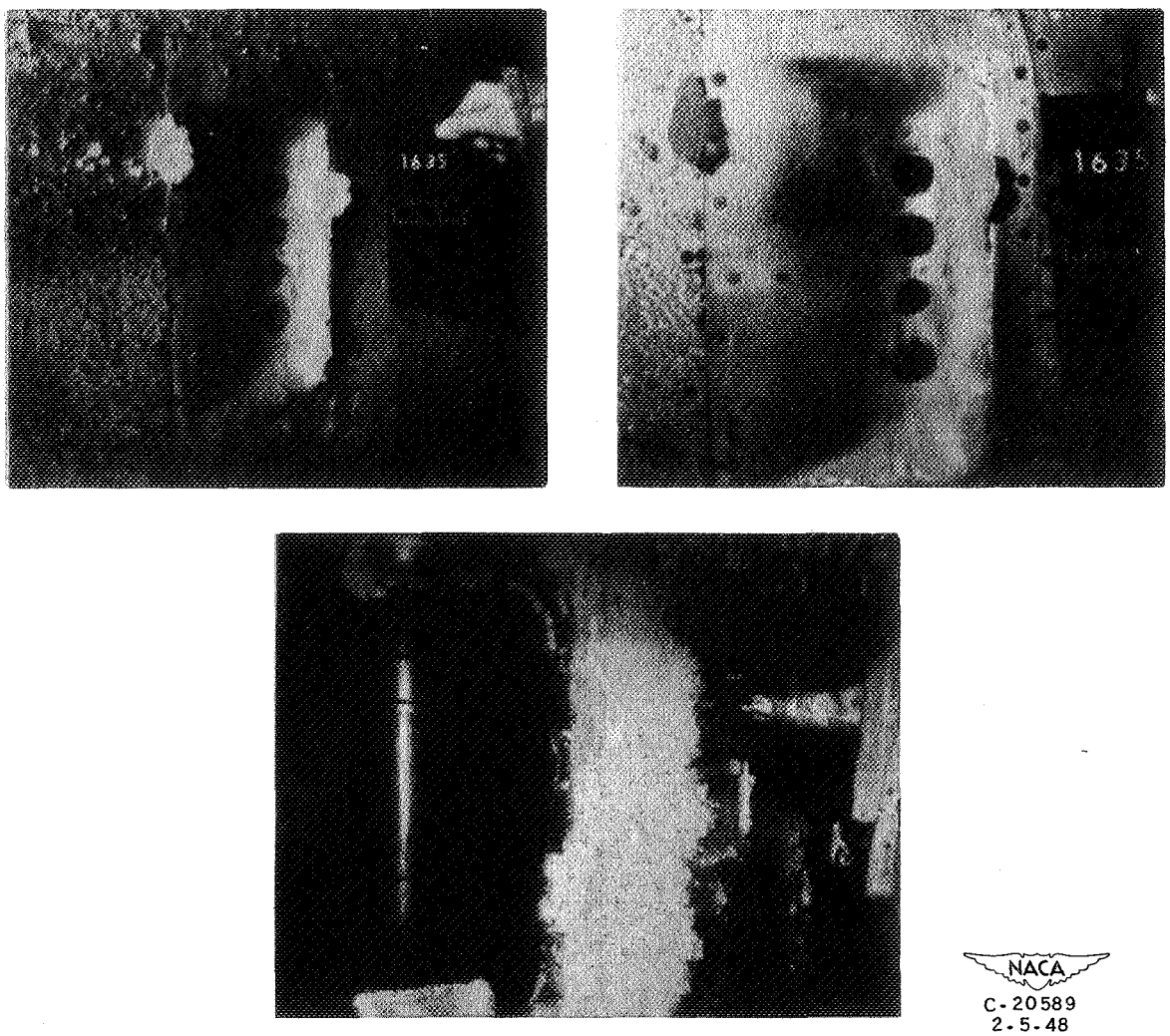

C-20589
2-5-48

Figure 12. - Ice formations on airfoil surface and configuration B following 35-minute freezing-rain experiment. Tunnel-air velocity, 240 feet per second; angle of attack, 16°; ambient-air temperature, 23° F; liquid-water content, approximately 1.8 grams per cubic meter.

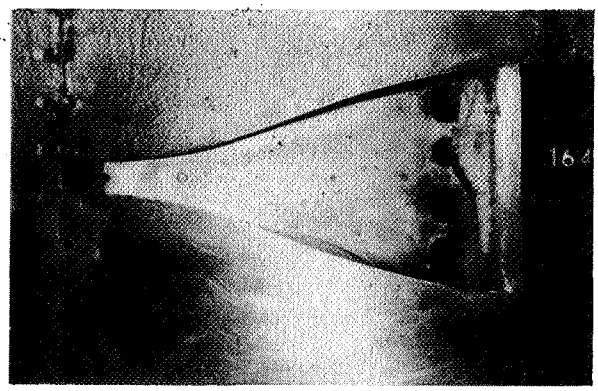

(a) Ice accretions following 15-minute icing period.

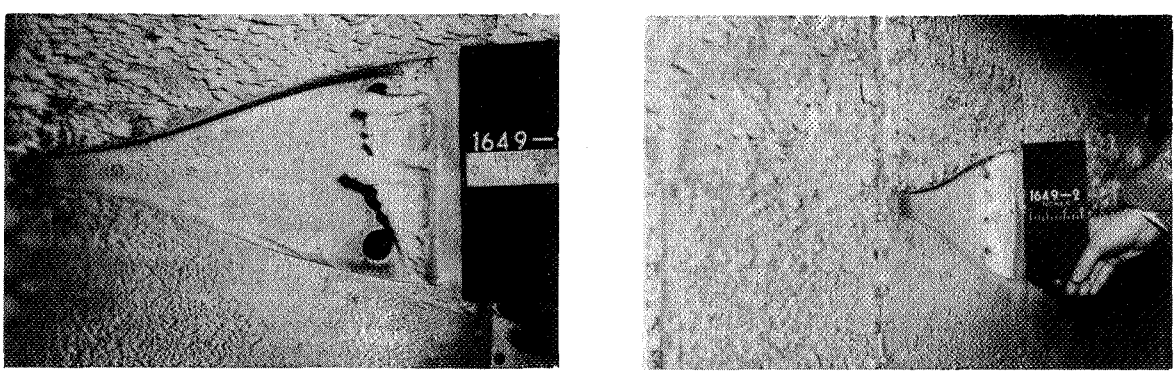

NACA
C-20856
3-9-48

(b) Ice accretions following 45-minute icing period.

Figure 13. - Ice formations on Configuration C. Tunnel-air velocity, 230 feet per second; angle of attack, 14°; ambient-air temperature, 20° F; liquid-water content, 1.5 grams per cubic meter.

1033

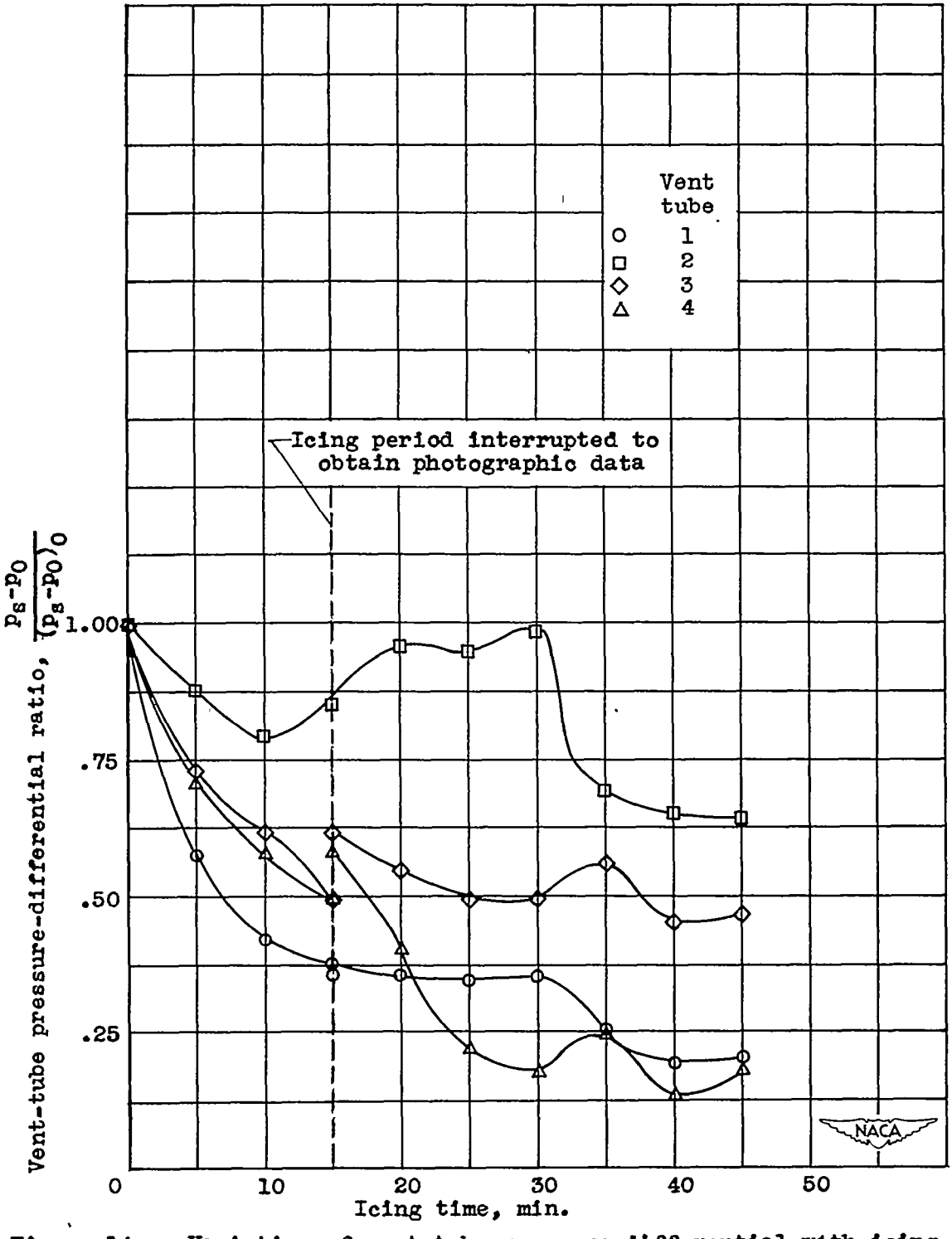

Figure 14. - Variation of vent-tube pressure differential with icing time for 45-minute icing period with configuration C. Average $(p_s-p_0)_0$, 5.1 inches water; tunnel-air velocity, 230 feet per second; angle of attack, 14°; ambient-air temperature, 20° F; liquid-water content, 1.5 grams per cubic meter.

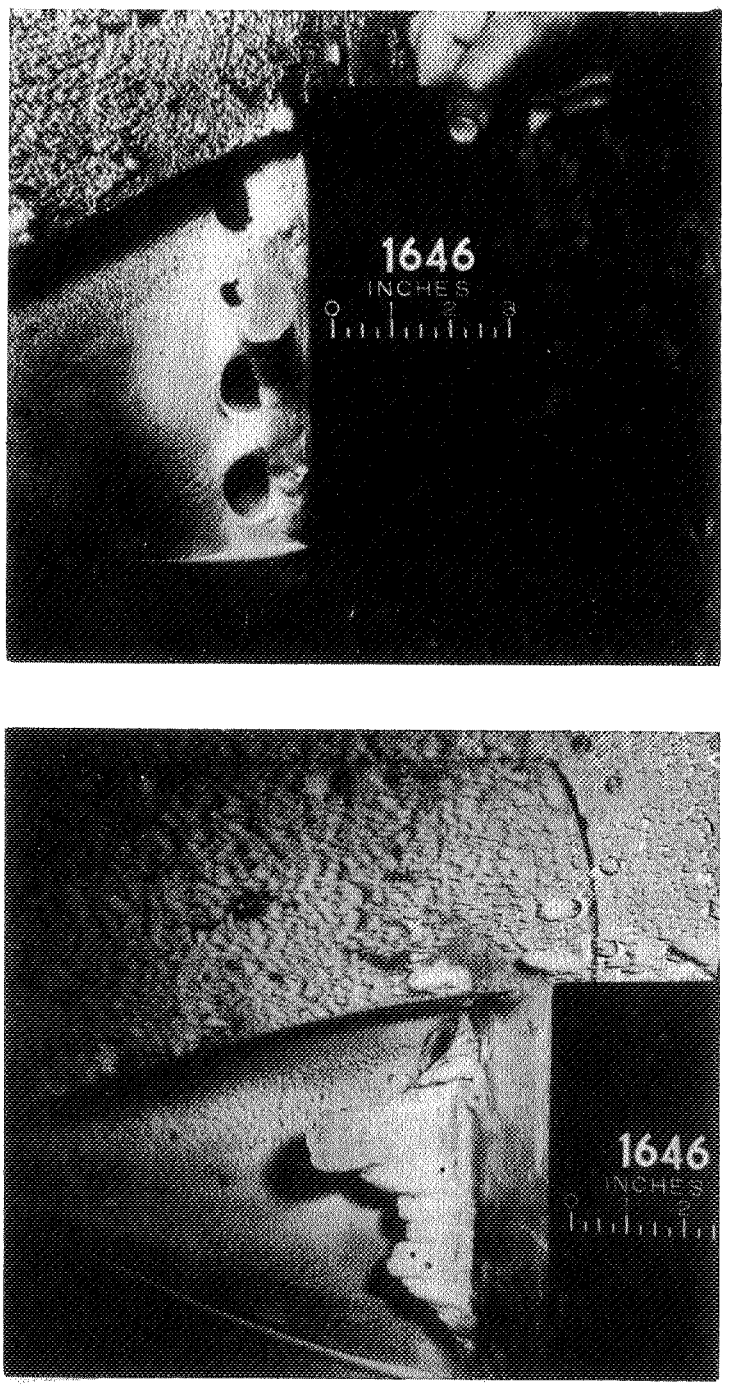

(a) Ice accretions following 30-minute icing period.

Figure 15. - Ice formations on configuration D. Tunnel-air velocity, 240 feet per second; angle of attack 14°; ambient-air temperature, 20° F; liquid-water content, 1.5 grams per cubic meter.

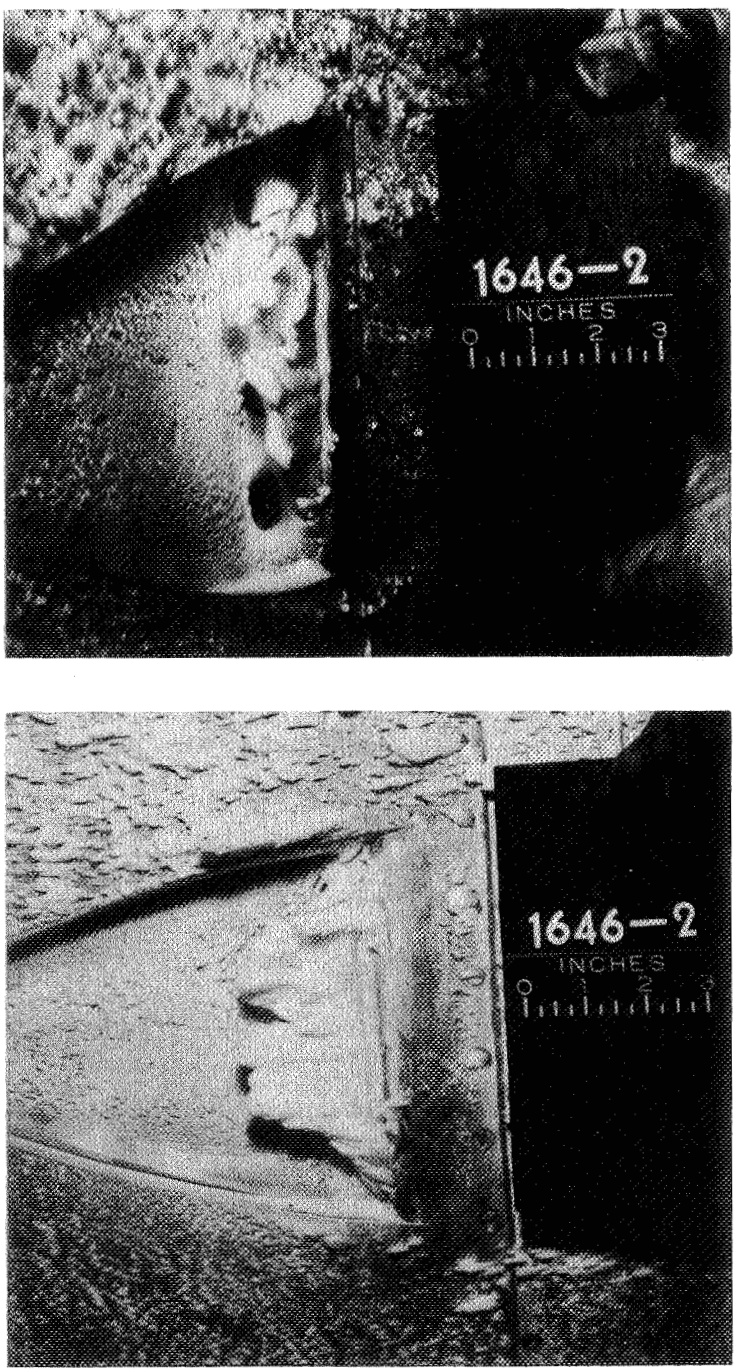

NACA
C-20855
3-9-48

(b) Ice accretions following 60-minute icing period.

Figure 15. - Concluded. Ice formations on configuration D. Tunnel-air velocity, 240 feet per second; angle of attack, 14°; ambient-air temperature, 20° F; liquid-water content, 1.5 grams per cubic meter.

1033

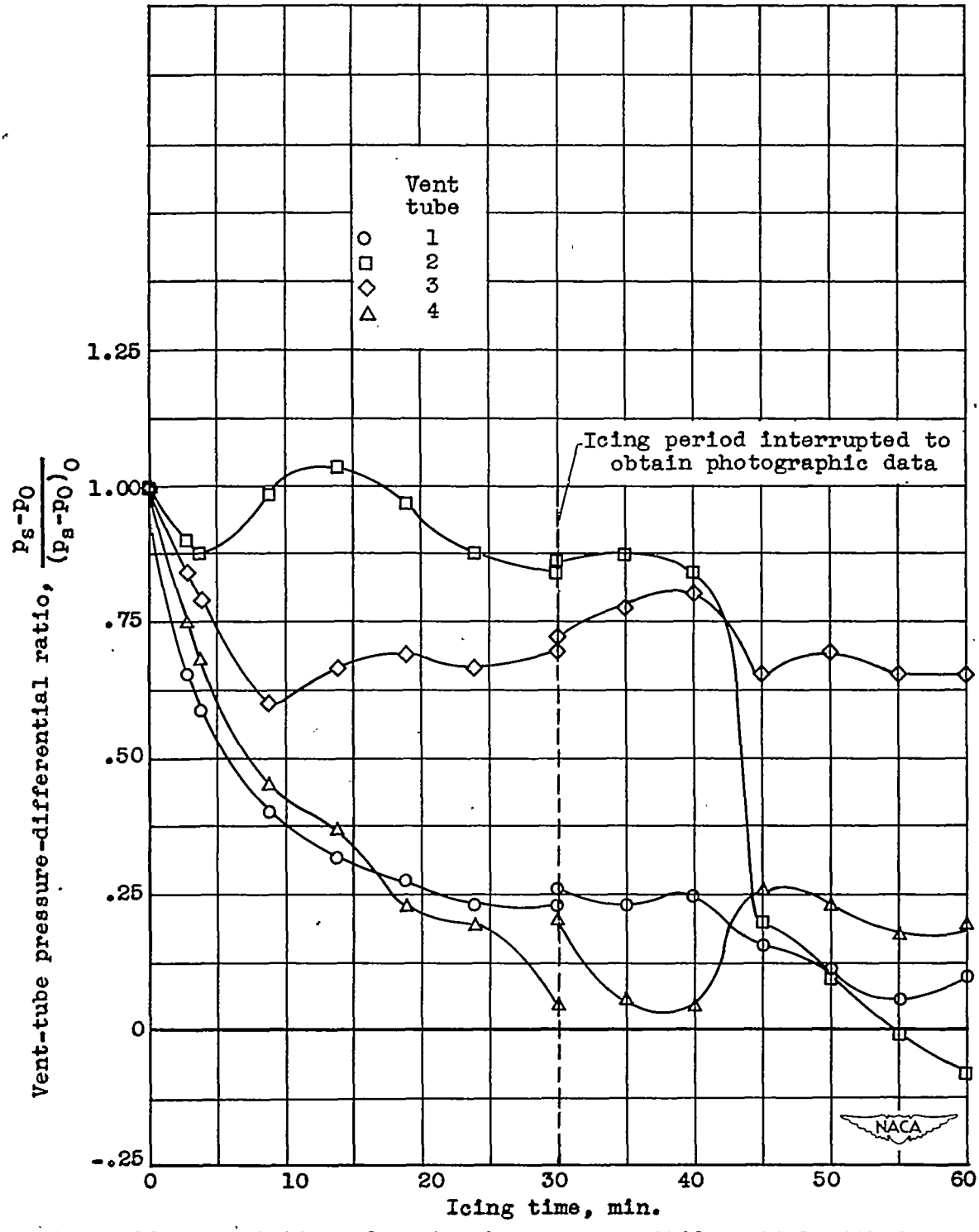

Figure 16. - Variation of vent-tube pressure differential with icing time for 60-minute icing period with configuration D. Average $(p_s-p_0)_0$, 6.9 inches water; tunnel-air velocity, 240 feet per second; angle of attack, 14°; ambient-air temperature, 20° F; liquid-water content, 1.5 grams per cubic meter.

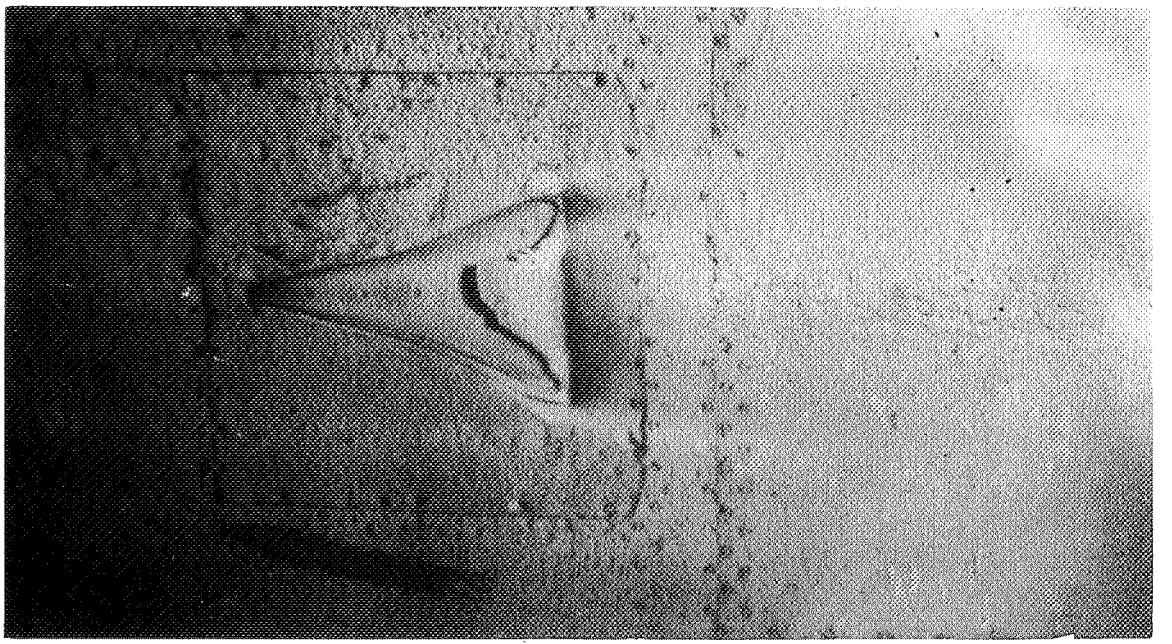

(a) Ice accretions following 47-minute icing period.

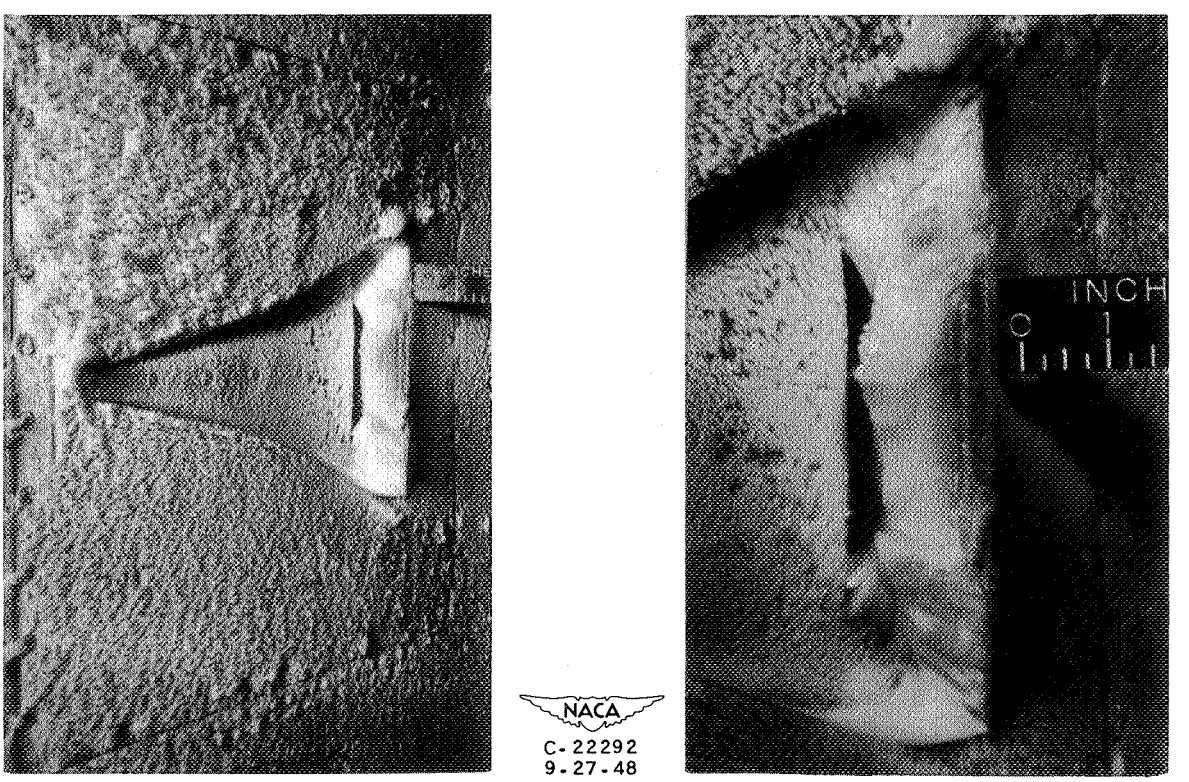

(b) Ice accretions following 60-minute icing period.

Figure 17. - Ice formations on configuration E. Tunnel-air velocity, 235 feet per second; angle of attack, 14°; ambient-air temperature, 21° F; liquid-water content, 1.1 grams per cubic meter.

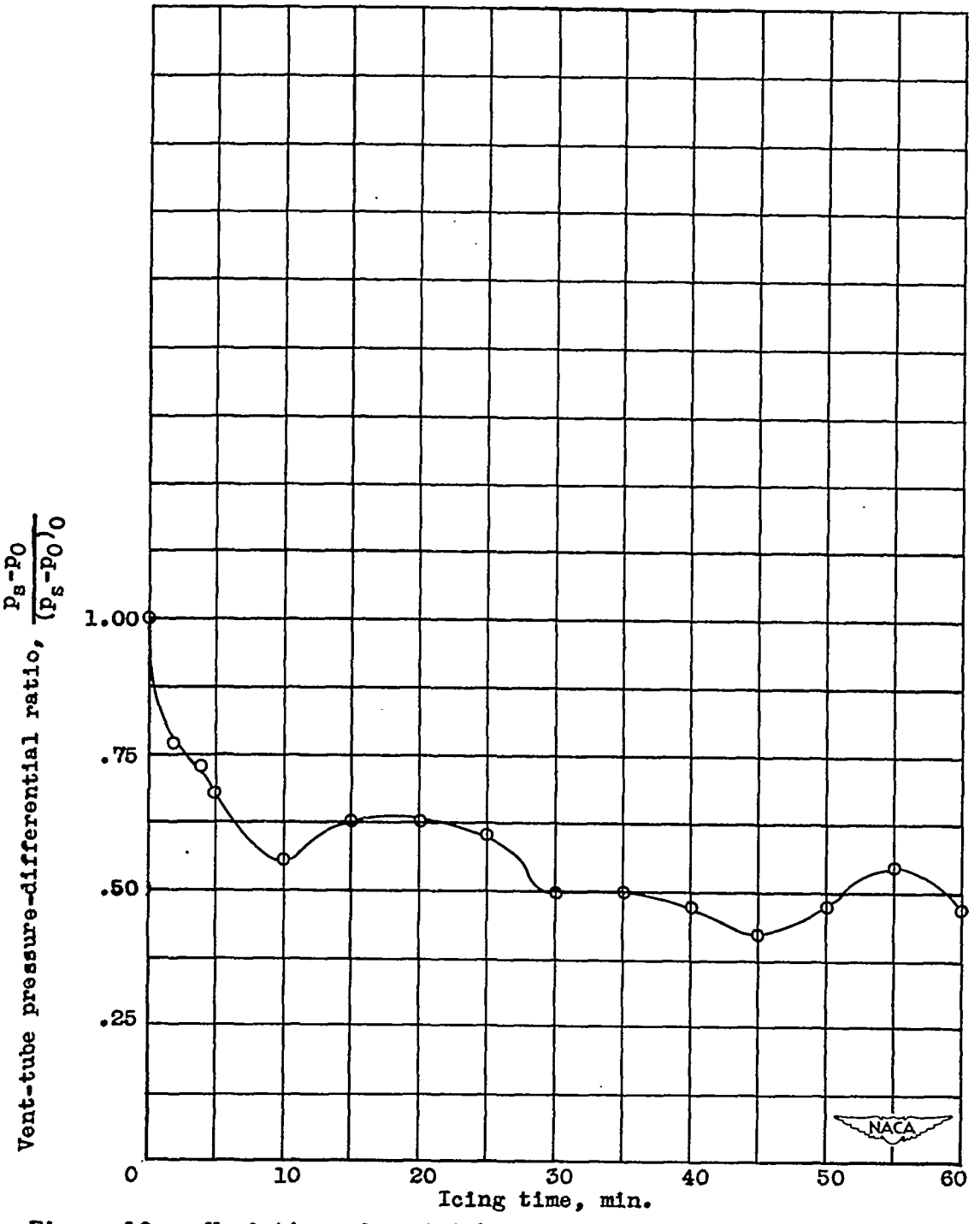

Figure 18. - Variation of vent-tube pressure differential with time for 60-minute icing period with configuration E. Average $(p_s-p_0)_0$, 7.6 inches water; tunnel-air velocity, 235 feet per second; angle of attack, 14°; ambient-air temperature, 21° F; liquid-water content, 1.1 grams per cubic meter.

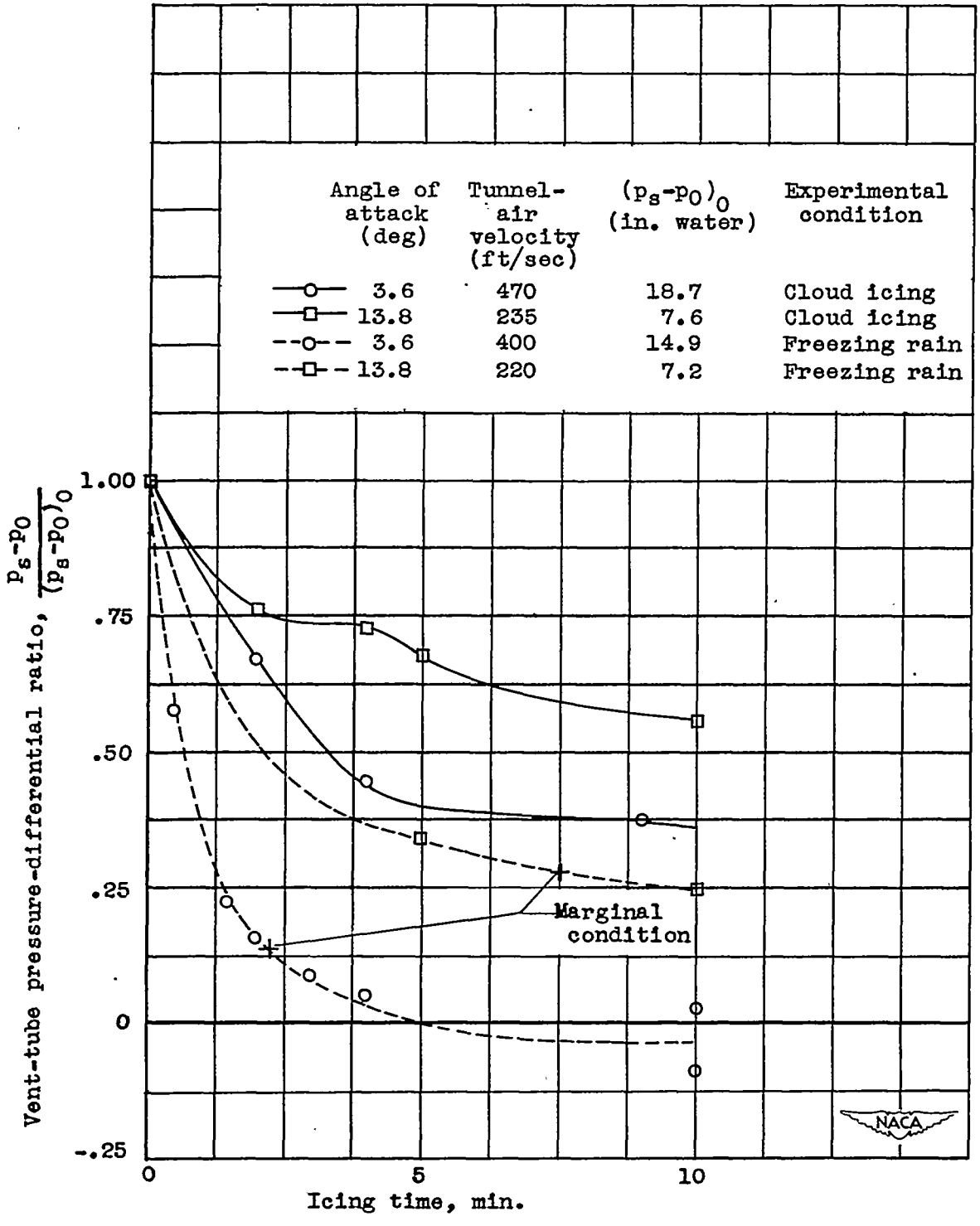

Figure 19. - Comparison of variation of configuration E vent-tube pressures with time for freezing-rain and cloud-icing conditions. Icing period, 10 minutes.

1033

1033

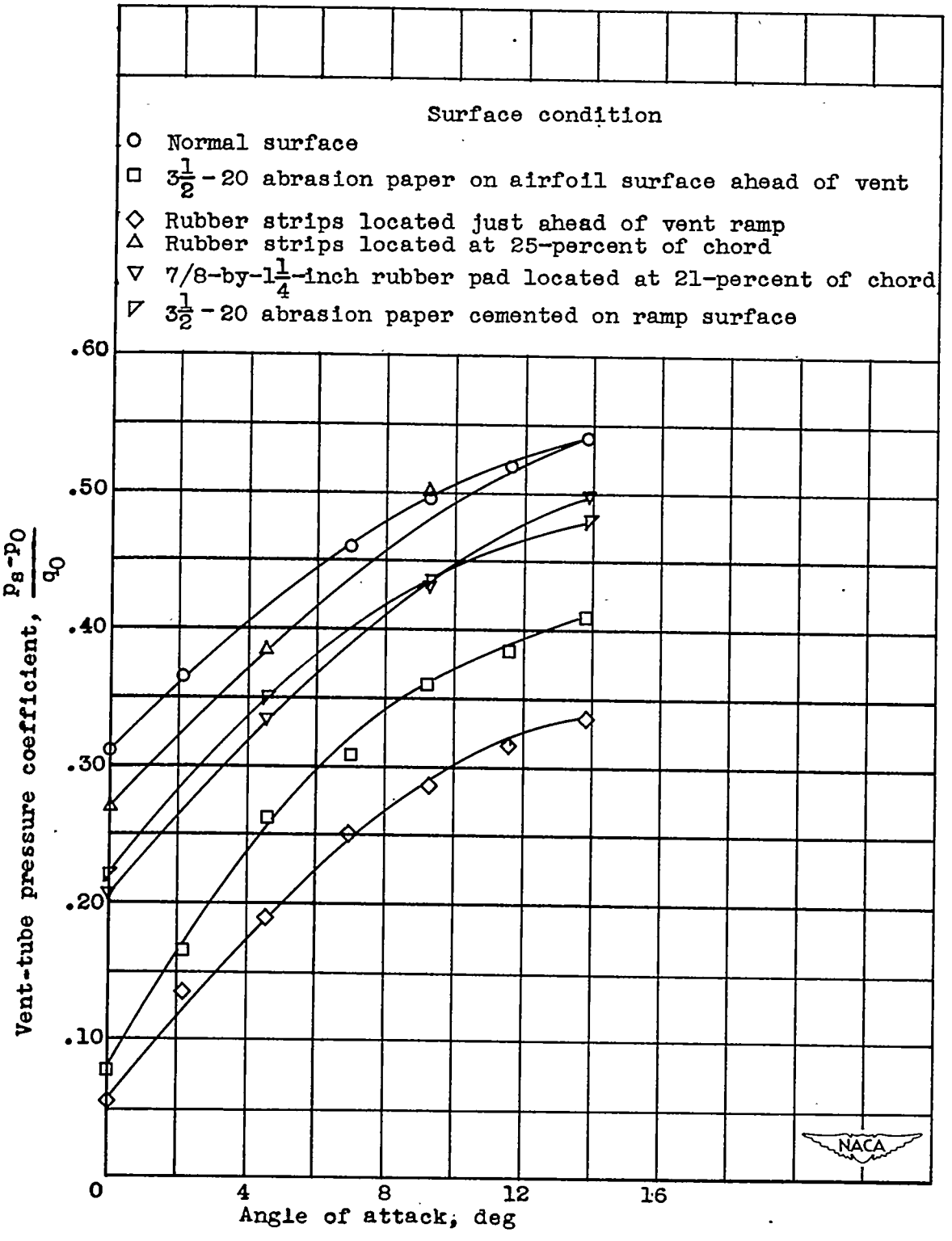

Figure 20. - Variation of vent-tube pressure coefficient with various types of surface roughness for configuration E.